Cite this: *Dalton Trans.*, 2017, **46**, 13562

Shortwave infrared luminescent Pt-nanowires: a mechanistic study of emission in solution and in the solid state†

Carl Cheadle,^a Jessica Ratcliff,^a Mikhail Berezin,^{*b} Vadim Pal'shin,^c Victor N. Nemykin ^d and Nikolay N. Gerasimchuk ^{*a}

Several complexes of "PtL₂" composition containing two cyanoxime anions – 2-oximino-2-cyano-*N*-piperidineacetamide (PiPCO[−]) and 2-oximino-2-cyano-*N*-morpholyacetamide (MCO[−]) – have been obtained and characterized both in solution and in the solid state. Complexes exist as two distinct polymorphs: monomeric yellow complexes and dark-green [PtL₂]_{*n*} 1D polymers, while for the MCO[−] anion a red, solvent containing dimeric [Pt(MCO)₂·DMSO]₂ complex has also been isolated. The interconversion of polymorphs was investigated. The monomeric PtL₂ units are arranged into anisotropic extended solid [PtL₂]_{*n*} polymers with the help of Pt...Pt metallophilic interactions. Crystal structures of monomeric PtL₂ (L = PiPCO[−], MCO[−]) and red dimeric [Pt(MCO)₂·DMSO]₂ complexes were determined and revealed the *cis*-arrangement of cyanoxime anions. The Pt–Pt distance in the "head-to-tail" red dimer was found to be 3.133 Å. The structure of the polymeric [Pt(PiPCO)₂]_{*n*} compound was elucidated using the EXAFS method and evidenced the formation of Pt-wires with ~3.15 Å intermetallic separation. The EPR spectra of both 1D polymers at variable temperatures indicate the absence of Pt(III) species. Both pure dark-green [PtL₂]_{*n*} polymers showed a considerable room temperature electrical conductivity of 20–30 S cm^{−1}, which evidences the formation of a mixed valence Pt(II)/Pt(IV) system. We discovered that these 1D polymeric [PtL₂]_{*n*} complexes show an intense NIR fluorescence beyond 1000 nm, while yellow monomeric PtL₂ complexes are not emissive at all. The room temperature excitation spectra of 1D polymeric [PtL₂]_{*n*} complexes demonstrated their strong emission beyond 1000 nm regardless of the used excitation wavelength between 350 and 800 nm, which is typical of systems with delocalized charge carriers. For the first time the formation of mixed valence "metal wires" held together by metallophilic interactions is directly linked both with an intense fluorescence in the NIR region of the spectrum and with the electrical conductivity. The effect of the concentration of [PtL₂]_{*n*} complexes dispersed in the dielectric salt matrix on the photoluminescence wavelength and intensity was investigated. Both polymers show a quantum yield that is remarkably high for this region of the spectrum, reaching ~2%. Variable temperature emission of polymeric [PtL₂]_{*n*} in the −190–+60 °C range was studied as well.

Received 26th June 2017,
Accepted 6th September 2017

DOI: 10.1039/c7dt02317k

rsc.li/dalton

Introduction

There is continuous interest in one-dimensional (1D) "metal wires" bearing a variety of organic and inorganic ligands and transition metals.^{1,2} Many of these numerous coordination polymers are held together *via* metallophilic interactions and also represent mixed valence systems.³ Their classification and properties were outlined in the pioneering work of Robin and Day,^{4,5} Allen and Hush,^{6,7} and Fackler,⁸ and summarized by Terril and Murray.⁹ In mixed valence complexes a low energy barrier between two different oxidation states provides the condition for electron transitions (hopping)⁹ induced by light or temperature. Solids that exhibit substantial conductivity represent systems with delocalized bonding^{3–5} (type III), and com-

^aDepartment of Chemistry, Temple Hall 431, Missouri State University, Springfield, MO 65897, USA. E-mail: NNGerasimchuk@MissouriState.edu

^bDepartment of Radiology, Washington University School of Medicine, St. Louis, MO 63110, USA. E-mail: berezinm@mir.wustl.edu

^cJ. Bennett Johnston Sr., Center for Advanced Microstructures & Devices, Louisiana State University, 6980 Jefferson Hwy, Baton Rouge, LA 70806, USA

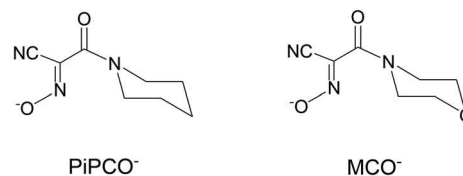
^dDepartment of Chemistry, University of Manitoba, Winnipeg, MB R3T 2N2, Canada

† Electronic supplementary information (ESI) available: Both CIFs and checkCIF reports for the discussed crystal structures. CCDC 1451036 – Pt(MCO)₂, 1451037 – Pt(PiPCO)₂, and 1451035 – [Pt(MCO)₂(DMSO)]₂. For ESI and crystallographic data in CIF or other electronic format see DOI: 10.1039/C7DT02317K

monly have an intense color (or metallic shine), and charge-transfer bands in the visible or near infrared (NIR) region.¹⁰ The prime interest in these systems has been driven by the fact that the major obstacle to a further decrease in the size of miniature electronic devices is heat dissipation, since conventional semiconductors require efficient cooling due to poor conductance and significant heat generation. Therefore, mixed valence compounds were extensively studied with the aim of exploring potential applications in molecular electronics due to their high electric conductance under ambient conditions. The mixed valence complexes with a two electron transfer often possess polymeric 1D columnar structures.^{11–14} These electrons are thought to have coherence similar to that of the Cooper pair, with Pt-based systems being studied the most.^{10,15–17} To date, there are two major types of conducting mixed valence Pt-based compounds known: MX complexes in which there are 50 : 50 mixtures of Pt(II)/Pt(IV) centers^{18,19} and KCP – classic cyano-platinates^{20,21} such as $K_2[Pt(CN)_4]Br_{0.3}$, Krogman's salt (or partially-oxidized cyano-platinates, POCP)¹⁰ (ESI 1⁺). Other platinum-based 1D solids include mixed valence polymeric oxalates,^{22,23} benzoquinon dioximes,^{24–26} and, more recently, dimethylglyoximates and their analogs.^{27–30} Blue Pt-pyrimidines and amidates,³¹ dimeric and trimeric complexes with similar ligands, were studied as well.^{32–35} The limited success achieved in the development of a molecular electric conductor based on the KCP and MX systems is attributed to the poor ligand design of these 1D metal–organic networks, insufficient control of the crystal architecture, and limited electronic tunability of the obtained systems. Thus, the MX and KCP complexes contain homogeneous donor atom sets: either $[PtN_4]$ or $[PtN_4X_2]$ (X = Cl, Br, I in MX solids), or $[PtC_4]$ (in KCP solids), or $[PtO_4]$ (in Pt-blue oxalates) in the metal center environment. The abovementioned Pt- α -dioximates also have a $[PtN_4]$ square-planar environment.^{24,26} The most important disadvantage of these systems from a chemical standpoint is their low solubility, which precluded the application of them as thin film conductors deposited on dielectric surfaces.

With the exception of several Pt(II) compounds obtained earlier for *in vitro* cytotoxicity testing,^{36–38} complexes of platinum with monoximes have never been systematically studied.

On the other hand, mixed valence complexes of Type II and Type III^{5,8} have been known to have low energy transitions in the red part of the electromagnetic spectrum including the NIR region. In the last decade, work on NIR technology opened up a variety of new ways in industrial, scientific, military and medical applications with new optical devices,^{39,40,92} imaging techniques^{41,42} contrast agents,^{43,44} and sensors.^{45,46} As a result of advances in new technology, a diverse range of photoluminescent compounds, emitting in the NIR region from small molecules to nanoparticles and larger aggregates, has emerged. The great majority of these materials, however, emit up to 850 nm while the number of NIR emitters with an emission beyond 900 nm is very limited. To the best of our knowledge no studies of emissive properties in that NIR region of mixed valence Pt-complexes have been carried out.



Scheme 1

Recently, we discovered six dark-green powdery Pt-cyanoximates that demonstrate temperature dependent strong emission beyond 900 nm in the NIR region.^{47,48}

Thus, our interest in mixed valence oxime-based coordination polymers of platinum is two-fold: (1) several Pt-cyanoximates have demonstrated significant *in vitro* cytotoxicity against human cancer cells at the level of cisplatin;^{36,38} (2) we recently discovered that one of those new Pt complexes with *N,N'*-diethylamino-2-oximino-2-cyanoacetamide (DECO)⁴⁸ self-assemble in solutions into 1D, intensely colored mixed valence species that are semiconductors under ambient conditions in the solid state. Therefore, these complexes can be viewed as suitable candidates for theranostic applications because they combine an imaging/diagnostic possibility and therapeutic potential. Here we extended our investigations to two other members of this family of Pt complexes.⁹³ In this paper we report the preparation and thorough characterization in the solid state and solutions of three soluble in organic solvents Pt-cyanoximates that contain anionic MCO⁻ and PiPCO⁻ ligands (Scheme 1). It should be noted that earlier we presented the synthesis and data of considerable biological activity of yellow monomeric Pt(MCO)₂ and Pt(PiPCO)₂ complexes.^{36–38} Their polymorphism and photophysical characteristics were unknown at that time.

Experimental section

General considerations

The common chemicals and solvents used were all of reagent grade (ALDRICH) and used without further purification. The TLC for ligand identification was carried out on silica-coated glass plates (Merck) with a 256 nm fluorescent indicator. Elemental analyses of C, H, and N content were performed at the Atlantic Microlab (Norcross, GA). Melting points were measured on Digimelt apparatus without correction.

Cyclic voltammetry (CV) and differential pulse voltammetry (DPV) studies

Electrochemical measurements were conducted using a CHI-620C electrochemical analyzer using the three-electrode scheme. Unless it is specifically mentioned, platinum working, platinum auxiliary and Ag/AgCl pseudo-reference electrodes were employed in a 0.1 M solution of TBAP in DMSO for electrochemical experiments. In all cases, the redox potentials are referenced to the FcH/FcH⁺ couple using ferrocene as an internal standard.

Dynamic light scattering

Particle size measurements during the course of the preparation of 1D polymeric complexes and for colloidal systems of $[\text{PtL}_2]_n$ ($L = \text{MCO}, \text{PiPCO}$) were carried out in organic solvents (spectral grade DMF, acetonitrile, and DMSO), and in micelles with the help of NanoBrook Omni apparatus from Brookhaven Inc. For these studies D_2O was used to eliminate possible absorbance of the NIR light with H_2O .

Micelles preparation

The micelles were formed after mixing fine powders of dark-green $[\text{PtL}_2]_n$ ($L = \text{MCO}, \text{PiPCO}$) complexes with a sodium decanoate, $\text{C}_9\text{H}_{19}\text{COONa}$ (C10), solution and a sodium dodecylsulfate, $\text{C}_{10}\text{H}_{21}\text{SO}_3\text{Na}$ (SDS), solution with the help of a Branson 1510 ultrasound bath for 5 minutes. All procedures were carried out at $+25^\circ\text{C}$. The amount of water used was 5 mL, and the amount of detergent used was ~ 20 mg. Micelles were left in the dark for a week and clear green solutions were pipetted for studies from small amounts of fine sediments at the bottom of the vial.

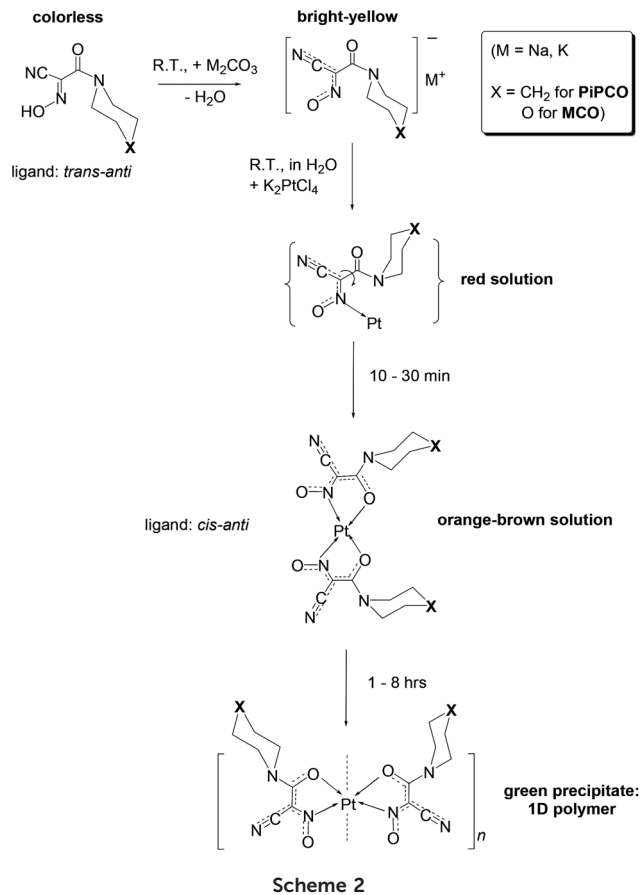
Pellets preparation

The KBr tablets for photophysical measurements were pressed as 13 mm disks from the thoroughly homogenized within 1 minute mixture of IR-spectroscopy grade KBr and the studied complexes in a stainless steel ball mill. Typical amounts of ingredients were 10 mg of PtL_2 complexes and 190 mg of dry KBr for 5% by weight concentration. For other, decreasing percentages of Pt-complexes in pellets, 10 mg of compounds were still used, but required larger amounts of KBr. A Carver hydraulic press at 23°C and a pressure of 9 metric tons (~ 6000 psi) was used to make these pellets.

Synthesis

The preparation of the two cyanoximes HPiPCO and HMCO was accomplished as previously described.³⁶ Both organic ligands represent white powders soluble in alcohols, CH_3CN , and acetone and sparingly soluble in water. Pure HPiPCO has m.p. = 151°C , $R_f = 0.31$ (EtOAc/hexane = 1 : 1), while HMCO has m.p. = 162°C and $R_f = 0.38$ in EtOAc/hexane = 2 : 1. The preparation of Pt-cyanoximates was carried out according to the two step method depicted in Scheme 2 using a slightly modified previously published procedure.⁴⁹ Syntheses were repeated five times with average yields of dark-green polymeric $[\text{PtL}_2]_n$ complexes ($L = \text{PiPCO}, \text{MCO}$) of 71% and 65%, respectively.

The typical preparation is reported for only one compound – $[\text{Pt}(\text{PiPCO})_2]_n$ – while the time course of the reactions was photo-documented as shown in ESI 2–4.† Thus, 0.2283 g (1.26 mM) of microcrystalline HPiPCO were placed in a beaker with 5 mL distilled water, and then 0.087 g (0.63 mM) of solid K_2CO_3 were added at once upon stirring. The reaction mixture immediately turned bright yellow and the white powder of HPiPCO dissolved with the formation of the K^+PiPCO^- solution and evolution of CO_2 . The solution was heated at first to ensure complete solubilization of the salt in water, and then



was filtered through a glass-wool plug. 0.2615 g (0.063 mM) of K_2PtCl_6 into 3 mL of water was added dropwise within 5 min to the above clear yellow solution of K^+PiPCO^- under stirring. The reaction mixture began to change the color and became turbid, and after ~ 1 hour a very fine dark-green precipitate became visible. It was left overnight at room temperature in the dark, followed by filtration and two times washing of the precipitate with 5 mL of water. $[\text{Pt}(\text{PiPCO})_2]_n$ was dried in a vacuum desiccator under $\text{H}_2\text{SO}_4(\text{c})$, giving 0.2458 g of the complex (71%). A very similar procedure was used for the preparation of $[\text{Pt}(\text{MCO})_2]_n$ with the amounts of reagents as: 0.2503 g (1.36 mM) of HMCO, 0.0944 g (0.68 mM) of K_2CO_3 , and 0.2836 g (0.68 mM) of K_2PtCl_4 ; the yield of the dark-green solid was 65% (0.2483 g). For $\text{C}_{16}\text{H}_{20}\text{N}_6\text{O}_4\text{Pt} - \text{Pt}(\text{PiPCO})_2$ – calculated (found), %: C – 34.60 (33.67), H – 3.63 (3.66), N – 15.13 (14.66). For $\text{C}_{14}\text{H}_{16}\text{N}_6\text{O}_4\text{Pt} - \text{Pt}(\text{MCO})_2$ – calculated (found), %: C – 30.06 (29.38), H – 2.88 (2.97), N – 15.02 (14.40). Both complexes have very similar solubility in organic solvents (ESI 5 and 6†) and are thermally stable to $\sim 170^\circ\text{C}$ (ESI 7 and 8†).

The preparation of the red dimer – $[\text{Pt}(\text{MCO})_2 \cdot (\text{DMSO})_2]_2$ – was carried out from dark-green $[\text{Pt}(\text{MCO})_2]_n$, 0.242 mg, upon dissolution in pure DMSO (1 mL) at $\sim 45^\circ\text{C}$. The initial green solution slowly became yellow and after an overnight slow cooling in a thermostat, the fine red needles of the dimer were collected on a filter paper. The complex is not very stable and, after a day, red needles become yellow (a monomeric complex

with no solvent in the lattice). All the operations and handling of this complex must be expeditious. Its identity was confirmed by the X-ray analysis.

The synthesis of the yellow monomeric Pt(PiPCO)₂ and Pt(MCO)₂ was carried out from the dark-green polymeric complexes in a pure DMSO/DMF = 1:1 mixture. After the compounds' dissolution the color of the mixture turned yellow, and after several weeks in the dark in a vacuum desiccator, a small amount of nice yellow needles of both complexes was collected on a filter paper and dried. The analytical data for monomeric Pt(PiPCO)₂ and Pt(MCO)₂ correspond to their formulas satisfactorily and the identity of these complexes was additionally confirmed by the X-ray analysis. Thus, for the yellow Pt(MCO)₂, C₁₄H₁₆N₆O₆Pt, calculated (found), %: C – 30.06 (29.71), H – 2.88 (2.93), N – 15.02 (14.82). Similarly, for the yellow Pt(PiPCO)₂, C₁₆H₂₀N₆O₄Pt, calculated (found), %: C – 34.60 (34.72), H – 3.63 (3.80), N – 15.13 (15.04). This complex is slightly hygroscopic.

Safety note. Although we have not encountered any problems during many years of laboratory work and handling, special care should be taken during work with platinum compounds because of their toxicity typical of heavy metals and especially cytotoxicity. Many platinum sources are water-soluble compounds and that emphasizes the absolute necessity for wearing protective gloves at all times when working with them.

Spectroscopic studies

IR-spectroscopy. The IR-spectra of all compounds reported herein were recorded in KBr disks at room temperature using a Bruker R70 FT-IR-Raman spectrophotometer. The spectra were acquired with 64 repetitions at a resolution of 4 cm⁻¹.

Mass spectrometry. The high-resolution electro-spray ionization mass spectra were recorded using a Bruker MicrOTOF-III system for samples of 1D polymeric [PtL₂]_n complexes (L = PiPCO, MCO) quickly after mixing them with CH₃CN under ambient conditions. The actual mass spectra and their analysis are presented in ESI 9–16.†

UV-Visible spectra. The electronic spectra of the compounds were recorded at room temperature using an HP 8354 diode array UV-visible spectrophotometer operating in the range of 200–1100 nm. The absorbance spectra from samples were measured in solutions and in fine suspensions squeezed between 1 × 4 cm quartz plates.

Emission spectra. The photoluminescence (PL) of the solid metal complexes was investigated using the following experimental setup: a Horiba model spectrofluorimeter using a CCD liquid-nitrogen-cooled InGaAs diode array camera (Symphony, Horiba) sensitive in the 600–1600 nm range and various integration times not exceeding 5 seconds. In the emission and excitation experiments both slits (emission and excitation) were kept constant at a width of 10 nm. The excitation was conducted with a Xe-lamp using a double grating (2 × 1200 g mm⁻¹ at 500 mm) monochromator. A long band pass 830 nm Schott RG 830 filter was placed in front of the spectrograph iHR-820 with a grating of 100 g mm⁻¹ at 800 mm. The

system was calibrated with a special glass standard (Nd doped) with well-known peak positions used for laser wavelength checking in the system before every set of measurements (ESI 21†). A custom-built anodized aluminum vacuum pumped cryostat filled with liquid N₂ was used for the variable temperature experiments in the –195/+70 °C range (ESI 17†). Prior to each cryogenic experiment, the emission from the empty cryostat itself (cold finger insert, clear adhesive tape, cardboard, windows, etc.) and KBr pellets was carefully examined to avoid artifacts associated with possible emissive contamination (ESI 20 and 21†). A J-Kem Scientific digital thermometer with a T-type thermocouple was used to monitor the temperature. The 3D excitation–emission scans of the tablets (KBr matrix with 5% of metal complexes) were recorded with the simultaneous measurement of the light intensity (*R*) and correcting the emission by the lamp light intensity (*T*₁). The absolute emission quantum yield of tablets with polymeric Pt-cyanoximates was measured using a large 150 mm (6 inch) integrating sphere and a fiber optic bundle with high transmission in NIR. The tablet was placed at the bottom-loading circular shallow drawer in the sphere.

All glassware cuvettes and hardware parts that were in contact with either KBr pellets or powders of the studied metal complexes were washed using DMF warmed to ~65 °C followed by DI water to avoid contamination and exclude the misinterpretation of the results of the photoluminescence measurements related to it. All synthesized complexes are well soluble in DMF.

NIR imaging. Images of pure solid powders of [PtL₂]_n (L = MCO, PiPCO) and KBr pellets containing different concentrations of both complexes (0.1, 0.5, 1 and 5 wt%) were obtained with the help of a Ninnox image camera and Nikkor lens 1:28, long pass 800 nm filter. Photographs were taken with illumination (excitation) using a 735 nm bright LED source from Thorlabs. The exposure time was set in all the experiments at 0.5 s and the sensor temperature at –15 °C.

Electron paramagnetic resonance (EPR). Spectra were recorded on a Bruker EMXplus X-band EPR spectrometer with a dual mode cavity and an Oxford cryostat system at +20 and –193 °C using the field sweep from 200 to 4000 G. The field was calibrated using DFPG, while the sensitivity of the instrument was checked using the standard of a solid solution of Al₂(SO₄)₃ containing 1% of Cr³⁺ centers as co-crystallized Cr₂(SO₄)₃. The spectra were recorded as the sum of five repetitions with the time constant for each of them set at 160 ms. Some of the spectra are presented in ESI 22.†

Structural studies

EXAFS data. A sample of polymeric [Pt(PiPCO)₂]_n in ~250 mg quantity was investigated at Louisiana State University in J.B. Johnston Sr. Center for Advanced Microstructures and Devices (CAMD). Data fitting and calculations were carried out using the FEFF8.4 software package.

X-ray crystallography. The crystal structures were determined for the yellow monomeric Pt(MCO)₂ and Pt(PiPCO)₂, and the red [Pt(MCO)₂(DMSO)]₂ dimer. Suitable single crystals of the first two complexes were grown by a slow ether vapor diffusion

method in CH₃CN solutions, while red needles of the dimer were obtained overnight from a concentrated Pt(MCO)₂ solution in DMSO. All attempts to grow suitable crystals of the dark-green polymeric [PtL₂]_n complexes (L = PiPCO⁻, MCO⁻) were unsuccessful (ESI 23†). The crystals of all yellow monomeric Pt(PiPCO)₂ were very thin and small and even at 120 s per exposure the value of *R*(int) was high: 0.24. Nevertheless, it was possible to successfully solve and refine the structure of this complex. Crystals of the red [Pt(MCO)₂(DMSO)]₂ dimer were too small to study using Mo-radiation and were sent to a synchrotron facility at the University of California-Berkeley to be studied as part of the SCrALS (Service Crystallography at Advanced Light Source) program. Crystallographic data were collected at Beamline 11.3.1 at the Advanced Light Source (ALS), Lawrence Berkeley National Laboratory. All the crystals were placed on plastic MiTeGen holders attached to the copper-pin positioned on the goniometer head of a Bruker APEX-2 diffractometer equipped with a SMART CCD area detector. The intensity data were collected at room and low temperatures in order to examine the possibility of temperature-dependent polymorphism that has been recently observed

in other Pt-cyanoximates,⁵⁰ but was not observed in the complexes presented in this work. Only low temperature data are presented in this work. Data collection was done in the ω scan mode using a Mo tube (K α radiation; λ = 0.71073 Å) with a highly oriented graphite monochromator. Intensities were integrated from 4 series of 364 exposures, each covering 0.5° in ω at 20–90 seconds acquisition time, with the total data set being a sphere. The space group determination was done with the aid of XPREP software. The absorption correction was performed by a crystal face indexing procedure with the help of a videomicroscope followed by numerical input into the SADABS program that was included in the Bruker AXS software package. All structures were solved by direct methods and refined by least squares on weighted *F*² values for all reflections using the SHELXTL program. In all structures H-atoms were placed at calculated positions in accordance with the hybridization state of a hosting carbon atom and were refined isotropically. No apparent problems or complications were encountered during the structures' solutions and refinement. The crystal data for Pt(MCO)₂, Pt(PiPCO)₂, and [Pt(MCO)₂(DMSO)]₂ are summarized in Table 1, with selected

Table 1 Crystal and refinement data for the studied Pt-cyanoximates: Pt(PiPCO)₂, Pt(MCO)₂ and its dimeric DMSO solvate

	Pt(MCO) ₂ , monomer	[Pt(MCO) ₂ (DMSO)] ₂ , dimer	Pt(PiPCO) ₂ , monomer
Empirical formula	C ₁₄ H ₁₆ N ₆ O ₆ Pt	C ₁₆ H ₂₂ N ₆ O ₇ PtS	C ₁₆ H ₂₀ N ₆ O ₄ Pt
F.W., g mol ⁻¹	559.42 g mol ⁻¹	637.54	555.47
Color	Yellow	Red	Yellow
Crystal size, mm	0.077 × 0.152 × 0.226	0.010 × 0.010 × 0.170	0.071 × 0.079 × 0.194
Temperature, K	120(2)	150(2)	100(2)
Crystal system	Triclinic	Triclinic	Orthorhombic
Space group, #	<i>P</i> $\bar{1}$, #2	<i>P</i> $\bar{1}$, #2	<i>P</i> bca, #61
Unit cell, Å, °	<i>a</i> = 6.6507(5) <i>b</i> = 8.7986(7) <i>c</i> = 15.4740(12) α = 94.2700(10) β = 96.0640(10) γ = 106.4490(10)	<i>a</i> = 6.8051(9) <i>b</i> = 13.6157(17) <i>c</i> = 24.278(3) α = 76.5560(10) β = 89.595(2) γ = 75.966(2)	<i>a</i> = 6.6743(10) <i>b</i> = 17.455(3) <i>c</i> = 30.557(5) α = 90 β = 90 γ = 90
Unit cell volume, Å ³	858.38(12)	2119.7(5)	3559.9(10)
<i>Z</i>	2	4	8
Density (calc.), Mg m ⁻³	2.164 g cm ⁻³	1.998	2.073
Absorp. coeff., mm ⁻¹	8.221	11.730	7.920
<i>F</i> (000)	536	1240	2144
θ range, °	1.33 to 25.00°	2.55 to 33.58°	2.33 to 27.18°
Index ranges	-7 ≤ <i>h</i> ≤ 7 -10 ≤ <i>k</i> ≤ 10 -18 ≤ <i>l</i> ≤ 18	-8 ≤ <i>h</i> ≤ 8 -16 ≤ <i>k</i> ≤ 16 -29 ≤ <i>l</i> ≤ 29	-8 ≤ <i>h</i> ≤ 8 -22 ≤ <i>k</i> ≤ 22 -39 ≤ <i>l</i> ≤ 39
Structure solution		<i>Direct</i>	
Reflections collected	8966	18 231	41 767
Independent reflections	3014 [<i>R</i> (int) = 0.0282]	8171 [<i>R</i> (int) = 0.0579]	3958 [<i>R</i> (int) = 0.2445]
Completeness to θ , (%)	25.00° (99.8)	33.58° (94.5)	27.18 (98.7)
Absorption correction	Multi-scan	Multi-scan	Multi-scan
<i>T</i> _{max} and <i>T</i> _{min}	1.0000 and 0.7794	0.8170 and 0.7110	0.7455 and 0.5492
Refinement method		<i>Full-matrix least-squares on F</i> ²	
Data/restraints/parameters	3014/0/244	8171/0/563	3958/36/245
Goodness-of-fit on <i>F</i> ²	1.043	1.010	0.980
Final <i>R</i> indices [<i>I</i> > 2 σ (<i>I</i>)]	<i>R</i> ₁ = 0.0193, <i>wR</i> ₂ = 0.0352	<i>R</i> ₁ = 0.0451 <i>wR</i> ₂ = 0.1366	<i>R</i> ₁ = 0.0538, <i>wR</i> ₂ = 0.1076
<i>R</i> indices (all data)	<i>R</i> ₁ = 0.0217 <i>wR</i> ₂ = 0.0359	<i>R</i> ₁ = 0.0480 <i>wR</i> ₂ = 0.1391	<i>wR</i> ₁ = 0.1267 <i>wR</i> ₂ = 0.1385
Largest peak/hole, e Å ⁻³	0.737 and -1.368	1.153 and -1.546	1.845 and -2.153
Extinction coefficient	n/a	n/a	0.0023(2)
Structure volume, Å ³ (%)	565.7 (65.3)	1379.9 (65.1)	2309.3 (64.9)

Table 2 Selected bond distances (Å) and angles (°) in the structure of monomeric yellow Pt-cyanoximates

Pt(PiPCO) ₂			
Bonds		Angles	
Pt(1)–O(2)	2.005(8)	N(1)–C(1)–C(3)	114.1(10)
Pt(1)–O(4)	2.000(8)	C(1)–C(3)–O(2)	115.7(10)
Pt(1)–N(1)	1.984(10)	N(4)–C(9)–C(11)	112.2(10)
Pt(1)–N(4)	1.939(10)	C(9)–C(11)–O(4)	115.5(10)
O(2)–C(3)	1.271(13)	O(2)–Pt(1)–N(1)	79.6(4)
O(4)–C(11)	1.305(14)	O(2)–Pt(1)–O(4)	95.3(3)
N(1)–O(1)	1.270(13)	N(1)–Pt(1)–N(4)	104.1(4)
N(4)–O(3)	1.257(11)		
N(1)–C(1)	1.307(16)		
N(4)–C(9)	1.382(14)		
C(1)–C(2)	1.454(17)		
C(9)–C(10)	1.429(17)		
C(2)–N(2)	1.130(16)		
C(10)–N(5)	1.154(15)		

Pt(MCO) ₂			
Pt(1)–O(3)	2.027(2)	O(3)–C(3)–C(1)	116.7(3)
Pt(1)–O(6)	2.019(2)	C(3)–C(1)–N(1)	114.1(3)
Pt(1)–N(1)	1.957(3)	O(6)–C(10)–C(8)	116.0(3)
Pt(1)–N(4)	1.962(3)	O(10)–C(8)–N(4)	113.9(3)
N(1)–O(1)	1.246(3)	O(3)–Pt(1)–N(1)	81.25(11)
N(4)–O(4)	1.257(3)	O(3)–Pt(1)–O(6)	95.89(9)
N(1)–C(1)	1.361(4)	N(1)–Pt(1)–N(4)	102.51(12)
N(4)–C(8)	1.355(4)		
C(1)–C(2)	1.428(5)		
C(8)–C(9)	1.427(5)		
C(1)–C(3)	1.453(5)		
C(8)–C(10)	1.455(5)		

bond lengths and valence angles presented in Table 2. The details of the crystal packing for these three complexes are presented in ESI 24–32.† A representative drawing of the crystal structures and packing diagrams was prepared using the ORTEP and Mercury software packages. Reported structures have been deposited at the CCDC with the following numbers: Pt(MCO)₂ – 1451036, Pt(PiPCO)₂ – 1451037, and [Pt(MCO)₂(DMSO)]₂ – 1451035,† with PLATON checkCIF reports without A- and B-type alerts.

Electron microscopy. Scanning Electron Microscopy (SEM) analysis for powders of dark-green [PtL₂]_n complexes (L = PiPCO, MCO) was carried out on a JEOL JSM-6320F field emission apparatus operated at 5 kV. Actual photographs are presented in ESI 34–38.†

Solid state electrical conductivity. Measurements for the fine powders of dark-green [PtL₂]_n complexes (L = PiPCO, MCO) were carried out using the Dimension 3100 SPM + C-AFM module with a platinum-iridium (PtIr) coated cantilever with a spring constant of 0.25 N m⁻¹ (SCM-PIC by Veeco). The contact area was 19.5 nm²; the scanning rate was set at 1 Hz, while the sample bias voltage was 50 mV. The complexes' film thickness was 264 nm for [Pt(MCO)₂]_n and 216 nm for [Pt(PiPCO)₂]_n. The obtained AFM images and specific details of these experiments can be found in ESI 40–42.†

Results and discussion

Synthesis

The protonated cyanoximes HPiPCO and HMCO are poorly water soluble and don't react in a reasonable time frame (days) with the K₂PtCl₄ that was used as a Pt-source. Thus, at first, aqueous solutions containing PiPCO⁻ and MCO⁻ anions, which are much better nucleophiles, have to be prepared (Scheme 2; ESI 2, 43 and 45†). Addition of stoichiometric amounts of K₂PtCl₄ leads to solid [PtL₂]_n complexes (L = PiPCO⁻ and MCO⁻ anions) as unusual dark-green precipitates within several hours. At first, monomeric PtL₂ complexes are formed, and quickly dimerize and polymerize into poor water soluble [PtL₂]_n nano-size aggregates that form opaque colloid systems (ESI 47†). A very fine dark-green solid eventually precipitated after the particles reached ~1 μm size (Scheme 2). It was not possible to stop the reaction at the stage of formation of the monomer or dimer and isolate these species in the direct reaction. The monomers of PtL₂, however, can be obtained from a dry solid polymeric [PtL₂]_n which forms upon reactions with an excess of donor solvent such as DMSO or DMF at elevated (~50 °C) temperatures. Therefore, a yellow monomer and a dark-green polymer represent true Pt(MCO)₂ and Pt(PiPCO)₂ polymorphs since they have the same chemical composition. The course of the reactions of the [PtL₂]_n complex (L = PiPCO, MCO) formation was monitored using the dynamic light-scattering technique as shown in Fig. 1 and in ESI 47 and 48.† A rather linear graph of the increase of the particles' size with time evidences the addition of the monomers to both ends of the growing polymer chain that is associated with "Ostwald ripening".⁵¹ The red colored dimeric [Pt(MCO)₂(DMSO)]₂ was isolated upon careful dissolution of dark-green [Pt(MCO)₂]_n in a small amount of DMSO at room temperature. The dimeric complex is technically not the polymorph of [Pt(MCO)₂]_n because of the presence of the solvent molecule in the structure, albeit not coordinated to the metal

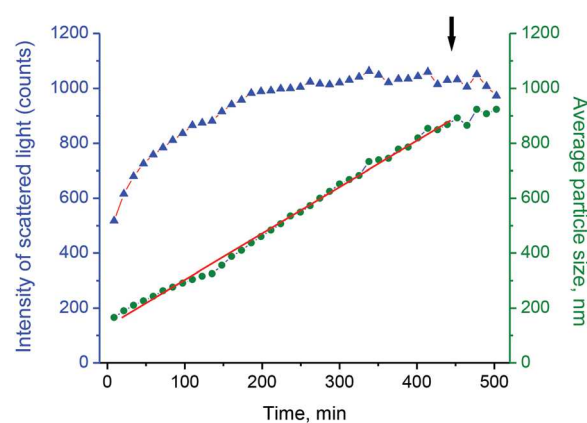


Fig. 1 Time profile of the formation of an emerald-green opalescent colloidal solution of [Pt(PiPCO)₂]_n after its dissolution in dry N,N'-dimethylacetamide, DMAA. An arrow indicates appearance of visible precipitate particles, while the red line shows their linear size growth consistent with "Ostwald ripening" in extended chain systems.

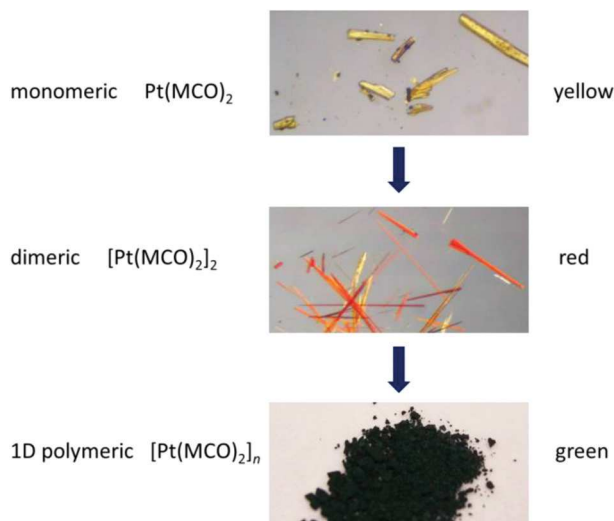


Fig. 2 Three polymorphs in the Pt-MCO system. The 1D coordination polymer is the only major bulk product of the reaction, while other forms can be isolated after its treatment with donor solvents which disrupt Pt...Pt interactions.

center. Nevertheless, for a better description of the structures and properties of the synthesized complexes in the $\text{Pt}^{2+}\text{-MCO}^-$ system the red $[\text{Pt}(\text{MCO})_2\text{-DMSO}]_2$ complex is included as a logical intermediate species between the $\text{Pt}(\text{MCO})_2$ monomer and the $[\text{Pt}(\text{MCO})_2]_n$ polymer (Fig. 2).

In order to examine the role of atmospheric oxygen in the synthesis of the self-assembled dark-green polymeric $[\text{PtL}_2]_n$ complexes ($\text{L} = \text{PiPCO}, \text{MCO}$), we performed an anaerobic preparation of $[\text{Pt}(\text{PiPCO})_2]_n$ *in situ* using a specialty quartz cuvette (ESI 49†). Thus, in the separate compartments of this 1 cm path graded-seal cell, we kept an aqueous solution of K^+PiPCO^- and solid $\text{K}_2[\text{PtCl}_4]$, which after several freeze-thaw cycles were combined under a protective Ar atmosphere. The miniature magnetic stir bar allowed for a quick mixing of ingredients and the course of the reaction was monitored with the help of the UV-visible spectrophotometer (ESI 49†). After ~10 min the reaction mixture slowly changed color to green, and within an hour, a very fine dark-green precipitate was observed at a similar time to that for the reaction carried out under ambient conditions. The carefully filtered and dried powdery sample of $[\text{Pt}(\text{PiPCO})_2]_n$ obtained in anaerobic preparation also moderately conducts electricity similarly (yet to a lesser extent) to its aerobically-made analog. Therefore, for the formation of the mixed valence polymeric $[\text{Pt}(\text{PiPCO})_2]_n$, it is not necessary to have the presence of oxygen from the air. The cyanoxime can act as an oxidizer and partially oxidize $\text{Pt}(\text{II})$ to $\text{Pt}(\text{IV})$ since this class of organic molecules has an intermediate position between nitro- and amino-compounds (ESI 50†). For example, the nitrosodicyanomethanide $\text{ONC}(\text{CN})_2^-$ anion was successfully oxidized to the nitrodicyanomethanide $\text{ON}_2\text{C}(\text{CN})_2^-$,⁵² and reduced to the respective amine. Most likely, both O_2 from the air and the mild oxidizing power of the cyanoxime facilitate the formation of small amounts of $\text{Pt}(\text{IV})$

centers in aerobically made $[\text{Pt}(\text{PiPCO})_2]_n$. Another plausible explanation for the anaerobic formation of $\text{Pt}(\text{IV})$ species could be a minor disproportionation reaction: $2 \text{Pt}(\text{II}) \rightarrow \text{Pt}(\text{0}) + \text{Pt}(\text{IV})$. Reduced platinum(0) species being in solutions do not contaminate the main precipitate of polymeric complexes as is evident from their SEM studies (see the discussion below in the Solid state studies section). Finally, Pt compounds are known to be catalytically active and may cause the partial chemical transformation of cyanoximes into moieties able to generate $\text{Pt}(\text{IV})$ species. A variety of such reactions involving $\text{Pt}(\text{II})$ and oximes have been reported previously by Kukushkin⁹⁴ and Pombeiro.⁹⁵ In any case, the formation of “poker chip” stacks has a thermodynamic drive to lose electrons from some number of Pt-atoms: when the hole is formed on the $6d_{z^2}$ orbital, it creates favorable conditions for the electron “hopping” from neighboring metal centers to share their filled $6d_{z^2}$ orbitals, providing the delocalization of charge through larger groups of metal atoms in a “Pt-wire”. However, a detailed investigation of the role of oxidizers, disproportionation, as well as establishing the reactions’ stoichiometry and the product(s) of redox transformations, is out of the scope of this paper, but surely will be addressed in our future publications on that subject.

Solutions studies

Mass-spectrometric measurements. Synthesized dark-green polymeric $[\text{PtL}_2]_n$ complexes display interesting behavior upon treatment with different solvents: they either keep the color or change it to yellow (ESI 5 and 6†), which evidences the formation of monomeric PtL_2 species ($\text{L} = \text{PiPCO}, \text{MCO}$). The quick dissolution of $[\text{PtL}_2]_n$ in CH_3CN resulted in the formation of a solution that quickly changed color to a light salad-green, which was subjected to mass-spectrometric measurements with the data being presented in ESI 9–16.† It is apparent that the oligomers – up to tetramers – can be reliably detected, which directly supports the polymeric structure of the starting dark-green solids. The calculated and found masses of the observed fragments fit very well. Such extended aggregation and certainly the formation of coordination polymers can be explained through the realization of the mixed valence $\text{Pt}(\text{II})\cdots\text{Pt}(\text{IV})$ species in which electrons/holes are moving along the “metal wire” vector.

Aggregation/disaggregation studies. In dry CH_2Cl_2 , DMF, *N,N'*-dimethylacetamide (DMAA), CH_3CN and some other solvents, both complexes dissolve with the formation of clear green solutions (ESI 5 and 6†), which within minutes become opalescent due to the spontaneous aggregation of these complexes in these solvents to form extended “poker chip” structures. The aggregation leads to a clearly observable Tyndall effect both at ambient day light and in the dark (ESI 47†). The investigation of the aggregation of the complexes during synthesis was carried out using the dynamic light scattering (DLS) method and revealed the formation of particles of ~900 nm size during ~9.5 hours from the starting $\text{K}(\text{MCO})$ and $\text{K}(\text{PiPCO})$ and $\text{K}_2[\text{PtCl}_4]$ (Fig. 1; Scheme 1). The rate of the linear particle growth of polymeric $[\text{Pt}(\text{MCO})_2]_n$ and

$[\text{Pt}(\text{PiPCO})_2]_n$ was found to be in the range of 30.7–40.4 nm min^{-1} for both compounds in aqueous solutions. Since the X-ray structures of the dimeric $[\text{Pt}(\text{MCO})_2]_2$ complex (in its DMSO solvate) and the EXAFS studies of the $[\text{Pt}(\text{PiPCO})_2]_n$ complex generated quite a reasonable Pt...Pt separation within ~ 3.13 – 3.15 Å, it was possible to assess how many molecules self-assemble into the stack per unit of time. Thus, the growth of the 1D column of $[\text{PtL}_2]_n$ (L = MCO, PiPCO) can be estimated between 97 and 130 molecules per minute.⁸⁸

However, the synthesized polymeric $[\text{Pt}(\text{MCO})_2]_n$ and $[\text{Pt}(\text{PiPCO})_2]_n$ in strong donor solvents such as DMSO, Py, HMPA and picolines become yellow (ESI 48†). Similarly, the green aggregated solutions of the studied Pt-cyanoximes quickly become yellow upon the addition of a drop or two of these solvents (ESI 51 and 52†). Clearly, strong donor solvents disrupt the 1D structure in stacks held by metallophilic interactions and lead to the formation of monomeric complexes. Thus, the “blue” CT band above 700 nm quickly disappears from the UV-visible spectra of complexes upon the addition of DMSO or Py (ESI 51 and 52†). At the same time the addition of sterically hindered strong bases such as 2,6-dimethylpyridine and 2,4,6-trimethylpyridine to solutions of both $[\text{Pt}(\text{MCO})_2]_n$ and $[\text{Pt}(\text{PiPCO})_2]_n$ complexes in DMF, as expected, does not lead to the color change and their disaggregation. It is important to mention that yellow solutions of monomeric $\text{Pt}(\text{MCO})_2$ and $\text{Pt}(\text{PiPCO})_2$ upon drying generate the dark-green polymeric complexes again, which implies the reversibility of the aggregation/disaggregation processes as depicted in Scheme 3. Also, in some cases it was possible to observe on the walls of vials and beakers the minor presence of red microcrystals of a dimeric species.

Dark-green $[\text{PtL}_2]_n$ (L = MCO, PiPCO) can be easily solubilized in aqueous solutions *via* micelle formation with the help of $\text{C}_9\text{H}_{19}\text{COONa}$ (C10) and $\text{C}_{10}\text{H}_{21}\text{SO}_3\text{Na}$ (SDS) (ESI, 53 and 54†). The results of DLS measurements indicated surprising formation of a single-size micelle particles in the above solutions (ESI 55†). Thus, the average $[\text{Pt}(\text{MCO})_2]_n$ micelle size was found to be 323 nm, and with a Pt...Pt bond = 3.15 Å (according to EXAFS data) there are ~ 920 units in the stack. For $[\text{Pt}(\text{PiPCO})_2]_n$ micelles the average particle size was found to be 214 nm, which transforms to ~ 680 units in the stack. Micelles, however, contain more than one stack cross-aligned in such way that a spherical particle is formed. This arrangement

leads to rather significant Pt content in the micelles, which was confirmed by analyzing the total metal amount using the ICP method.

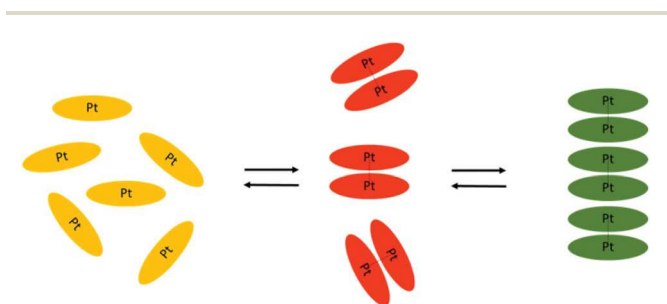
Electrochemical measurements. Redox properties of yellow solutions of the monomeric platinum complexes $\text{Pt}(\text{MCO})_2$ and $\text{Pt}(\text{PiPCO})_2$ along with the redox properties of the corresponding ligands were investigated using CV and DPV techniques and depicted in ESI 56–58.† In general, all redox processes both in ligands and in platinum complexes were found to be irreversible. The reduction potentials in all systems were close to each other and thus were assigned as the ligand-centered processes. The irreversible oxidation process in platinum complexes was observed at significantly lower potential as compared to the oxidation process observed in the corresponding ligands.

UV-visible spectra

Ligands. Both HMCO and HPiPCO cyanoximes are colorless compounds but gain a yellow color upon deprotonation. The UV-visible spectra of the cyanoxime anions MCO^- and PiPCO^- (as Na^+ , K^+ or alkylammonium salts) contain three bands: two for π – π^* transitions in the area of 200–300 nm and one low intensity $n \rightarrow \pi^*$ transition ($\epsilon \sim 80$ –100) which, depending on the solvent, is typically observed around 420 nm. The latter band is responsible for the yellow color of cyanoxime anions.^{53–56} That band also demonstrates a pronounced solvatochromism: of 86 nm for the MCO^- anion (4857 cm^{-1} , 56.5 kJ mol^{-1} , or 601 meV), and 87 nm (4996 cm^{-1} , 59.8 kJ mol^{-1} , or 619 meV) for the PiPCO^- between UV-visible spectra in water and DMSO, respectively (ESI 44–46†).

Metal complexes. We found that the complexes $[\text{Pt}(\text{MCO})_2]_n$ and $[\text{Pt}(\text{PiPCO})_2]_n$ slowly dissolve in organic solvents and can form solutions of two different colors: green and yellow depending on the solvent. The green color is a combination of yellow (from the $n \rightarrow \pi^*$ transition in the anion) and blue colors that originated as the result of a charge-transfer band between the Pt centers and cyanoximes in a stack.^{47,48} Polar donor solvents tend to quickly discolor green solutions into yellow, which indicates the disaggregation of the coordination polymers into yellow monomeric units $\text{Pt}(\text{MCO})_2$ and $\text{Pt}(\text{PiPCO})_2$ (ESI 48, 52 and 53†). Crystal structures of these have been determined (Fig. 3 and the discussion below).

There is a difference in the peak position between $[\text{Pt}(\text{MCO})_2]_n$ and $[\text{Pt}(\text{PiPCO})_2]_n$ in solutions with even more of a red shift of λ_{max} to 810 and 841 nm, respectively, as opposed to solid samples (see the discussion below). The origin of a further bathochromic shift of the blue bands is not clearly understood at the moment, but it could well be due to free “annealing” and reaching the most favorable equilibrated structures in the aggregated colloid solutions of 1D coordination polymers as opposed to solid samples. Moreover, we also observed rather significant solvent sensitive changes in the λ_{max} of the CT band in UV-visible spectra of the studied complexes in a series of organic solvents (ESI 59 and 60†). For $[\text{Pt}(\text{MCO})_2]_n$ the largest variance in λ_{max} was observed for



Scheme 3

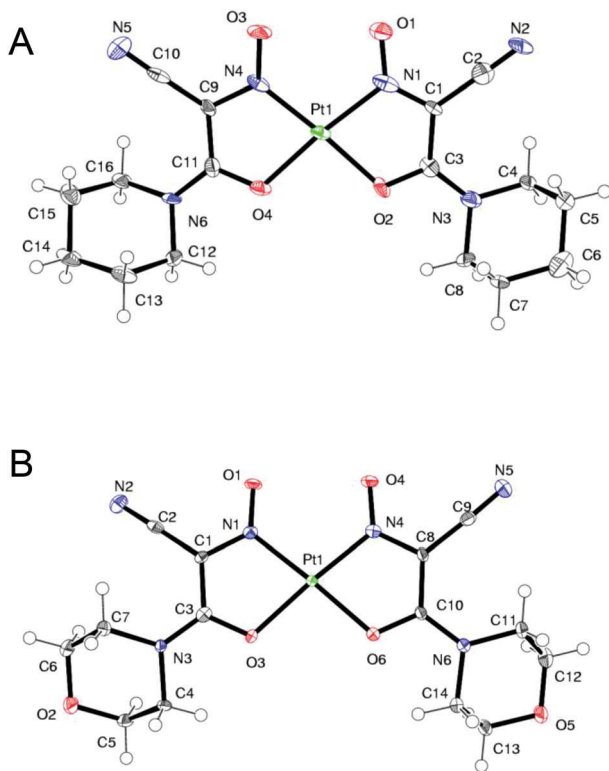


Fig. 3 Molecular structure and numbering scheme of monomeric Pt(II)-cyanoximates: A – top view of yellow Pt(PiPCO)₂; B – top view of yellow Pt(MCO)₂; an ORTEP drawings at the 50% thermal ellipsoids level.

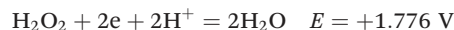
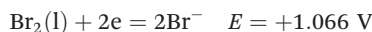
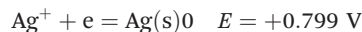
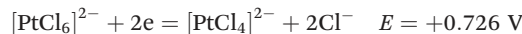
ethanol (765 nm) and DEAA (809 nm), giving a 45 nm difference that corresponds to an 8.69 kJ mol⁻¹ energy change (ESI 59†). The polymeric dark-green [Pt(PiPCO)₂]_n had a λ_{max} in formamide at 775 nm, while in ethyl acetate it is at 843 nm, which amounts to 74 nm or to a 13.66 kJ mol⁻¹ energy change (ESI 60†).

Thus, UV-visible spectroscopic studies of the solutions of dark-green 1D polymeric [Pt(MCO)₂]_n and [Pt(PiPCO)₂]_n in a large group of organic solvents allowed us to establish certain trends between Kosover's specific solvation energy,⁵⁷ solvent donor number and λ_{max} of the Pt...Pt CT band in the spectra (ESI 61†).

Other known dark-colored Pt-based coordination polymers are the Magnus' Green Salt (MGS), green Becton's Salt and purple Milton's Salt briefly described below. Those, however, have insufficient solubility in common solvents and have been poorly studied in general.

Chemical oxidation studies in solutions. Known Pt-based 1D solids, such as KCP-type M₂[Pt(CN)₄] (M = Na, K, Rb, Cs), were successfully converted into partially oxidized (POCP) mixed valence compounds in which up to 30% of the Pt-centers could become Pt(IV). These copper-like shiny crystalline complexes represent classic 1D solids that exhibit a strong optical anisotropy and conduct electricity at the level of metals. The oxidation of Pt(II) can be achieved either by electrochemical methods or by using chemical oxidizers such as Ag⁺, bromine

or H₂O₂, the standard half-reaction potentials^{58,59} of which are shown below.



The data of the solid state electrical conductivity measurements of our polymeric [PtL₂]_n (L = MCO⁻, PiPCO⁻ anions) complexes evidenced already the formation of a mixed valence species (see ESI 41 and 42,† and text below). Nevertheless, we were interested in the possibility of further chemical oxidation of the metal center of our Pt-cyanoximates in solutions to determine whether or not these compounds followed trends similar to classic POCP complexes.

Pt(MCO)₂. In order to prove the formation of mixed valence aggregated Pt-cyanoximates, we carried out the partial oxidation of the Pt(II) in solutions using oxidizers such as Ag⁺ and elemental bromine. For the oxidation of Pt(II) centers in the solid state, we used a 30% solution of H₂O₂. Thus, in a separate experiment, the stepwise addition of 1 and 2 equivalents of the AgPF₆ solution to a green aggregated solution of [Pt(MCO)₂]_n in DMF resulted in an increase of the intensity of the “blue” CT-band that is associated with the “poker chip” stacking of complexes and the formation of a mixed valence species (ESI 62-A†). Similarly, the addition of 0.2 equivalent of a Br₂ solution in dry DMF to a green aggregated solution of [Pt(PiPCO)₂]_n also produced a significant bathochromic shift of the “blue” band in the UV-visible spectra (ESI 62-B†). Therefore, both treatments evidenced the further oxidation of the Pt(II) centers to Pt(IV), in aggregated stacks, and more extensive formation of mixed valence species. Despite the good qualitative trend, we were not able, unfortunately, to isolate reproducibly and characterize products of the performed chemical oxidation of green [PtL₂]_n (L = MCO⁻, PiPCO⁻ anions) in solutions. A similar situation is known for the KCP solids where the generated mixed valence POCP complexes frequently have a variable, non-consistent composition that depends on “sample's history” and the methods of their preparation.⁸⁷

Pt(PiPCO)₂. A sample of [Pt(PiPCO)₂]_n was also oxidized with Br₂ in dimethyl formamide (DMF). Thus, 47.3 mg (0.076 mmol) of dark-green [Pt(PiPCO)₂]_n was mixed with 4.0 mL of DMF and placed under a N₂ atmosphere. Then 0.590 mL (0.023 mmol) of a 0.039 M Br₂ solution (in DMF) was added to the [Pt(PiPCO)₂]_n mixture and stored overnight under an argon atmosphere for 24 hours. Upon opening the reaction vessel, it was heated to 35 °C for one hour with inert gas purging to remove excess Br₂. A dark green solid was observed under a yellow solution. After drying under high vacuum, 25.6 mg of an olive-drab solid was recovered. The material had a slightly metallic, copper-like sheen.

The further oxidation of dark-green [Pt(PiPCO)₂]_n was also carried out by titration with AgPF₆ in DMF. Thus, 1.5 mL ali-

quots of 7.75×10^{-4} M of the Pt-complex solution (in DMF) were mixed with 23 μL aliquots of 2.65×10^{-2} M AgPF_6 solutions (in DMF as well) and monitored by UV-visible spectroscopy. An increase in the intensity of the Pt...Pt CT band at ~ 800 nm was observed, similarly to that for the $[\text{Pt}(\text{MCO})_2]_n$ complex above.

Chemical oxidation in the solid state. Bromine vapors were used to further oxidize and, therefore, introduce the Pt(IV) center solid $[\text{Pt}(\text{MCO})_2]_n$, which was embedded in the KBr pellet (5% by weight, for the photoluminescence experiments; see the NIR spectroscopy discussion below), to the mixed valence species. The photographs of the initial dark-green pellet and the one after exposure to Br_2 (copper-like shine) are presented in ESI 63.† Hydrogen peroxide, 30% by weight, was also successfully used to further generate mixed valence Pt-cyanoximate complexes that were incorporated into the KBr pellets at 5% concentrations (see the NIR experiments section). One drop of 10 μL of H_2O_2 applied on the surface of the pellet provided a significant NIR emission intensity increase. Therefore, the low energy photoluminescence of $[\text{PtL}_2]_n$ is directly associated with the formation of a mixed valence system.

Finally, the Pt-cyanoximates reported in this work resemble the previously studied Pt-based 1D solids^{5,21} in the sense of their ability to form mixed valence complexes. However, contrary to classic compounds such as MGS, Krogman's salt and its derivatives, our $[\text{PtL}_2]_n$ ($\text{L} = \text{MCO}^-$, PiPCO^- anions) complexes: (1) exhibit a significant photoluminescence beyond 1000 nm, and (2) are soluble in organic solvents.

Solid state studies

It is well known that the vast majority of Werner-type Pt(II) complexes with a variety of inorganic and organic ligands are colorless or have pale-yellow/off-white colors. There are only three intensely colored complexes: the Magnus' Green Salt (MGS)^{60,61} of "Pt(NH₃)₂Cl₂" composition, purple Millon's Salt $[\text{Cu}(\text{NH}_3)_4][\text{PtCl}_4]$, and green Becton's Salt $[\text{Pt}(\text{NH}_3)_4][\text{CuCl}_4]$.⁶² All have 1D polymeric stacked "poker-chips" type structures with alternating cationic $[\text{Pt}(\text{NH}_3)_4]^{2+}$, $[\text{Cu}(\text{NH}_3)_4]^{2+}$ and anionic $[\text{PtCl}_4]^{2-}$, $[\text{CuCl}_4]^{2-}$ units, respectively. Accordingly, these are considered as Pt...Pt and alternating Cu...Pt wires with intermetallic distances less than 3.4 Å. A very unusual and intense color of the obtained presented here Pt(II) cyanoximates indicates that they have similar structures and properties to those of anisotropic 1D solids.²¹

Structural studies

The crystal structures of both ligands – HMCO and HPiPCO – were determined in the past.^{36,63} These compounds were found to have two polymorphs: the HMCO crystallizes in two different orthorhombic polymorphs in a $P2_12_12_1$ space group, while HPiPCO can crystallize in either monoclinic⁶³ $P2_1/c$ or orthorhombic³⁶ $P2_12_12_1$ space groups. The crystal structures of three Pt-cyanoximates were determined using X-ray crystallography and the structure of one 1D-polymeric complex was elucidated by the EXAFS method. It should be mentioned that the structure of $\text{Pt}(\text{PiPCO})_2$ was determined earlier at 293 K, but

we re-grew suitable single crystals and re-determined the structure more accurately at low temperature (100 K) because of the recently observed polymorphism in other Pt-cyanoximates.⁵⁰

X-ray structures of yellow monomeric $\text{Pt}(\text{PiPCO})_2$ and $\text{Pt}(\text{MCO})_2$. The formation of yellow monomeric *cis*-complexes of the PtL_2 composition ($\text{L} = \text{PiPCO}$, MCO) as products of the breakdown of dark-green polymeric $[\text{PtL}_2]_n$ has been confirmed (Fig. 3).

Cyanoxime anions in both complexes adopt *cis-anti* configuration^{36,64} and are in the nitroso form as evident from much shorter N–O as C–N bonds in the C–N–O fragment (Table 2). The Pt(II) centers have a planar $[\text{PtN}_2\text{O}_2]$ environment with two shorter by ~ 0.06 Å *cis*-Pt–N bonds as compared to two *cis*-Pt–O bonds. Both anionic PiPCO^- and MCO^- cyanoximes form five-membered chelate rings with metal centers. The metal-cyanoxime core in both complexes is virtually planar, but has dihedral angles of 22–28° between the PtN_2O_2 five atom plane and piperidine and morpholine cycles (both in the chair form) attached to the amide groups (ESI 24 and 26†). The details of the crystal packing for both yellow monomeric $\text{Pt}(\text{PiPCO})_2$ and $\text{Pt}(\text{MCO})_2$ polymorphs are presented in ESI 25 and 27.†

X-ray structure of a red $[\text{Pt}(\text{MCO})_2\cdot\text{DMSO}]_2$ dimer. The structure of a red dimeric complex $[\text{Pt}(\text{MCO})_2\cdot\text{DMSO}]_2$ was found to consist of a dimeric head-to-tail $[\text{Pt}(\text{MCO})_2]_2\cdot\text{DMSO}$ moiety associated with the Pt(2) atom (Fig. 4), as well as slipped

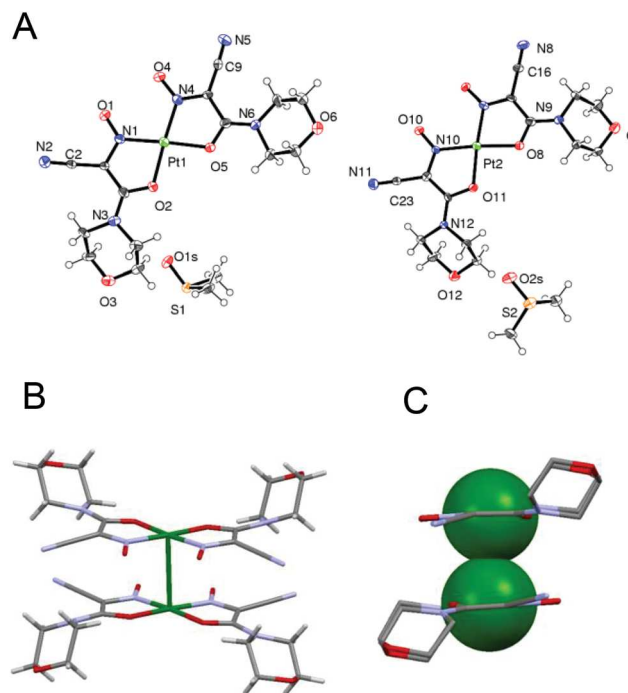


Fig. 4 The ASU in the structure of a red dimer $[\text{Pt}(\text{MCO})_2\cdot\text{DMSO}]_2$ showing two crystallographically different molecules (A). The Pt2-based monomer has a symmetry related (i) second part bound in a "head-to-tail" fashion (B) with a short connection between two Pt-centers at 3.133 Å (C, side view) shown in space-filling mode and with H atoms omitted for clarity.

Table 3 Selected bond distances (Å) and angles (°) in the structure of the dimeric part of red $[\text{Pt}(\text{MCO})_2\cdot\text{DMSO}]_2$, at the Pt(2) center

Bonds		Angles	
Pt(2)–O(8)	2.025(4)	N(10)–Pt(2)–N(7)	104.1(2)
Pt(2)–O(11)	2.016(4)	N(7)–Pt(2)–O(11)	174.83(18)
Pt(2)–N(7)	1.981(5)	N(7)–Pt(2)–O(8)	80.57(19)
Pt(2)–N(10)	1.979(5)	N(10)–Pt(2)–O(11)	81.03(18)
N(7)–O(7)	1.249(6)	N(10)–Pt(2)–O(8)	175.03(16)
N(10)–O(10)	1.236(6)	O(11)–Pt(2)–O(8)	94.26(17)
N(7)–C(15)	1.348(8)	O(7)–N(7)–C(15)	120.6(5)
C(15)–C(16)	1.444(8)	N(7)–C(15)–C(16)	117.5(5)
C(16)–N(8)	1.140(8)	N(7)–C(15)–C(17)	114.7(5)
C(15)–C(17)	1.446(8)	C(16)–C(15)–C(17)	127.4(6)
C(17)–N(9)	1.331(8)	O(8)–C(17)–N(9)	117.3(5)
C(17)–O(8)	1.285(7)	O(8)–C(17)–C(15)	116.7(5)
C(22)–N(10)	1.354(7)	N(9)–C(17)–C(15)	126.0(5)
C(22)–C(23)	1.445(8)	N(10)–C(22)–C(24)	114.7(5)
C(22)–C(24)	1.451(7)	N(10)–C(22)–C(23)	117.9(5)
C(23)–C(11)	1.132(8)	N(12)–C(24)–C(22)	125.6(5)
C(24)–O(11)	1.297(7)	O(11)–C(24)–N(12)	117.9(5)
C(24)–N(12)	1.332(7)	O(11)–C(24)–C(22)	116.4(5)

π -stacked columns of the $[\text{Pt}(\text{MCO})_2]\cdot\text{DMSO}$ complex with head-to-head oriented units associated with the Pt(1) atom (ESI 28, 31 and 32†). Two cyanoxime anions in both Pt(1) and Pt(2) centers form *cis*-complexes with planar $[\text{PtN}_2\text{O}_2]$ geometry with chelating ligands forming five-membered metallo-cycles (Fig. 4, Table 3; ESI 29†). The closest metal–metal distance in the dimeric part of the molecule was found to be 3.1335(5) Å.

The geometry of the cyanoxime anion in the dimer is very similar to that of the monomeric complex. The crystal packing of the dimeric $[\text{Pt}(\text{MCO})_2]\cdot\text{DMSO}$ moiety is described as a column of dimers extended along the *a*-direction (ESI 30†). Selected bonds and angles for the non-dimeric part of the structure at the Pt(1) center are presented in ESI 33.† The crystal packing for this part of the complex represents slipped zigzag stacks that also form a columnar structure, but with long distances between the metal centers (ESI 31 and 32†). Molecules of the DMSO are trapped in the structure and occupy channels along the *a*-direction (ESI 28 and 31†). This feature explains the instability of the dried red complex when it loses the solvent and changes to the yellow monomeric $\text{Pt}(\text{MCO})_2$. The solvent, associated with the dimeric part in the structure, formed interesting short electrostatic contacts between one of the DMSO methyl-groups and the oxygen atoms of the nitroso-groups of two cyanoximes: O8...H2C1 and O7...H2C1 equal to 2.520 and 2.547 Å, respectively.

EXAFS structure of 1D $[\text{Pt}(\text{PiPCO})_2]_n$. In order to elucidate the structure of these new types of compounds, we used the EXAFS method at the Pt-K edge, which allowed for the determination of the length of the chemical bonds around the heavy atom. The results of the EXAFS studies are shown in ESI 38 and 39† and demonstrate a very good fit (within 1–7% values) between the calculated and experimentally determined parameters of bond length and interatomic distances. The model used for the fit had a bidentate cyanoxime anion binding Pt, with the formation of a five-membered chelate ring in a

fashion similar to that found in $\text{Pd}(\text{II})^{36}$ and $\text{Ni}(\text{II})^{65}$ cyanoximates. Determined by the EXAFS method and data fitting, Pt–N and Pt–O bonds are slightly shorter than those experimentally observed in yellow monomeric $\text{Pt}(\text{PiPCO})_2$ and $\text{Pt}(\text{MCO})_2$ (Table 2), which may suggest rather tighter binding of the equatorial cyanoxime anion to the metal center in the dark-green 1D polymer. The intermetallic Pt...Pt separation established by EXAFS is 3.15 ± 0.1 Å (ESI 39†), which is in very good agreement with the commonly observed distances in established 1D Pt-based mixed valence electric conductors,^{10,13} as well as for the dimeric red $[\text{Pt}(\text{MCO})_2\cdot\text{DMSO}]_2$ complex discussed above. The determination of the Pt...Pt intermetallic distance in dark-green polymers was the prime goal for using the EXAFS method because we were unable to crystallize a suitable for the X-ray analysis specimen.

Known literature examples of complexes of platinum-based complexes with a variety of α -dioximes are presented in Table 4 which contains both polymeric and monomeric complexes and mixed valence systems as well. There is an almost exclusively $[\text{PtN}_4]$ coordination environment around the central atom in the displayed there complexes, whereas in our case we have a mixed donor atoms $[\text{N}_2\text{O}_2]$ surrounding of the central atom.

Scanning electron microscopy. Samples of dark-green fine powders of $[\text{Pt}(\text{PiPCO})_2]_n$ and $[\text{Pt}(\text{MCO})_2]_n$ polymers were studied at different magnification powers and the results are summarized in ESI 34–37.† The compounds represent fibrous, pure and homogeneous single phase materials without any observable phases of foreign impurities.

Electrical conductivity. The solid state conductivity measurements of the dark-green $[\text{Pt}(\text{PiPCO})_2]_n$ and $[\text{Pt}(\text{MCO})_2]_n$ polymers were found to be at the upper level of semiconductors with values of 22.2 and 33.3 S cm^{-1} , respectively (ESI 40–42†). This is direct evidence of the formation of a mixed valence species with free charge carriers moving along the Pt–Pt vector in these 1D solids.

Thermal stability. The synthesized dark-green $[\text{Pt}(\text{PiPCO})_2]_n$ and $[\text{Pt}(\text{MCO})_2]_n$ polymers are thermally stable up to 172 and 200 °C, respectively (ESI 7 and 8†). The final products of their decomposition are PtO_2 (at 1180 °C) for $[\text{Pt}(\text{PiPCO})_2]_n$ – 40.88% calculated (43.60% found), and Pt metal (at 980 °C) for $[\text{Pt}(\text{MCO})_2]_n$ – 35.12% calculated (35.12% found).

Spectroscopic data

EPR spectra. The spectra recorded at room temperature and 80 K from fine dark-green powders of $[\text{PtL}_2]_n$ complexes ($\text{L} = \text{PiPCO}^-$, MCO^-) demonstrated the absence of the signals of Pt^{3+} centers which have an EPR observable d^7 electronic configuration³¹ (ESI 22†). Therefore, the mixed valence species in the studied complexes belong to Pt(II)...Pt(IV) pairs with d^8 – d^6 electronic configurations. The same situation was also well documented for classic mixed valence MX and KCP/POCP 1D solids (ESI 1†) in the past.^{5,10,13,66}

UV-visible spectra. Solid samples of 1D polymeric Pt-cyanoximates appeared as fine dark green powders (Fig. 2; ESI 64†). Thus, fine suspensions of $[\text{Pt}(\text{MCO})_2]_n$ and $[\text{Pt}(\text{PiPCO})_2]_n$

Table 4 Literature data for the crystal structures of different Pt-oximates and Pt-oxalates

Complex	Oxime ligand	Color	Pt...Pt, Å	Space gr.	Comments	CCDC ref. code, ref.
Pt(GLY) ₂	1,2-Glyoxaldioxime	Brown-viol	3.506	<i>P2₁/n</i>	Columnar 1D structure overlaid stacks extended along the <i>a</i> direction	GLYOPT ²⁹
Pt(DMG) ₂	1,2-Dimethylglyoxime	Blue	3.257	<i>Ibam</i>	Columnar structure overlaid stacks extended along the <i>c</i> direction; 1D wire	PTNGLO01 ⁸⁰
Pt(DMG)·L ₂	1,2-Dimethylglyoxime (dicarb = dicarbene)		7.053	<i>P2₁/c</i>	Layered structure with a large offset of units to each other	HESWES ⁸¹
Pt ₃ (DMG) ₃ (OAc) ₄	1,2-Dimethylglyoxime (+ CH ₂ Cl ₂ solvent)		2.516 2.603 2.522	<i>P</i> $\bar{1}$	Isolated tri-Pt triangular motif with 2 bridging and 2 monodentate acetates: mixed valence system	MEMLEV ²⁶
Pt ₈ (DMG) ₇ (OAc) ₆	1,2-Dimethylglyoxime (+CH ₂ Cl ₂ solvent)		2.529 2.549 2.678	<i>P</i> $\bar{1}$	Octa-Pt assembly composed of two tetramers connected <i>via</i> a bridging DMG ligand; 6 chelating DMG ligands, and 5 bidentate OAc and 1 monodentate OAc groups: mixed valence system	MEMLUL ²⁶
Pt(DEG) ₂	1,2-Diethylglyoxime	Dark-brown	3.555	<i>C₂/c</i>	Slipped columnar structure extended along the <i>c</i> direction	KACPAF ²⁷
Pt(DPG) ₂	1,2-Diphenylglyoxime	Orange/black	3.260	<i>P4/ncc</i>	Columnar structure with stacks extended along <i>c</i> ; 1D wire	PGLXPT ⁶⁶
Pt(DCG) ₂	1,2-Dichloroglyoxime		3.176	<i>Iba2</i>	Columnar structure with stacks extended along <i>a</i> ; 1D wire	BOHWOK ⁸²

Literature data for different Pt-oximates and Pt-oxalates.

Complex	Oxime ligand	Color	Pt...Pt, Å	Space gr.	Comments	CCDC ref. code, ref.
Pt(BQD) ₂	1,2-Benzoquinone dioxime	Blue	3.173	<i>Ibam</i>	Columnar structure with stacks extended along <i>c</i> ; 1D wire	BQDXPT ²⁴
Pt ₃ (DMG) ₃ (OAc) ₄	1,2-Dimethylglyoxime,	Red-brown	2.259	<i>P</i> $\bar{1}$	Isolated tri-Pt triangular cluster with 2 bridging and 2 monodentate acetate groups: mixed valence system	WAGPUP ⁸³
Pt ₃ (NIOX) ₃ (OAc) ₄	1,2-Cyclohexyldioxime		2.542			
Pt(COG) ₂ Cl ₂	1,2-Cyclooctylglyoxime (Cl ⁻ bound to the metal)		2.696	<i>P2₁/n</i>	Discrete Pt(III) dimers	PALTOL ⁸⁴
Pt(DAG) ₂ ·H ₂ O	1,2-Diaminoglyoxime (I ⁻ and H ₂ O as well)	Red	3.242	<i>P</i> $\bar{1}$	Slipped columnar structure with stacks along the <i>a</i> direction: mixed valence system	DAXWAK ⁸⁵
Pt(DAG) ₂ ·Pt(Ox) ₂	1,2-Diaminoglyoxime (mixed-ligands complex)		3.660	<i>P2₁/n</i>	Slipped columnar structure with tilted alternating stacks along the <i>b</i> direction	DOGCAD ⁸⁶

contain intense bands at *ca.* 746 and 795 nm, respectively (Fig. 5). The presence of these “blue bands” was conveniently used during the preparation and handling of these complexes as an indication of the formation or presence of stacks of coordination polymers. The effect of aggregation in solution or the formation of a 1D-polymer in the solid state leads to a significant red shift of absorbance bands (and emission, respectively) as was proposed by Miskowski⁸⁹ and more concisely presented by Li *et al.*⁹⁰ In our case in the visible range a band at ~430 nm in yellow monomeric PtL₂ complexes shifts to ~550 nm in a dimer, and then to ~750 nm in a 1D polymer. The latter is assigned to $d\sigma^* \rightarrow \sigma(\pi^*)$ MMLCT.⁹⁰ Finally, based on the studies carried out,⁴⁸ the wavelength of 770 nm was selected as an excitation energy for recording the emission spectra of the solid 1D polymeric [Pt(MCO)₂]_n and [Pt(PiPCO)₂]_n which are presented below.

NIR spectroscopy

The most interesting property of the two dark-green [Pt(MCO)₂]_n and [Pt(PiPCO)₂]_n complexes was a strong emission in the NIR region beyond 1000 nm. The importance of

this part of the electromagnetic spectrum for biomedical research is outlined in ESI 65–68† and is associated with the tissue transparency between 1030 and 1100 nm. A combination of imaging potential with the established cytotoxicity of several Pt-cyanoximates^{36–38} opens the possibility for their theranostic applications. Recently, we reported the chemistry and photoluminescence properties of the first mixed valence Pt-cyanoximate.⁴⁸ Two other complexes presented in this work widen the series of newly discovered NIR emitters that could be useful for biomedical research.

The presence of absorption bands beyond 700 nm associated with aggregation *via* metallophilic interactions observable in the UV-visible spectra of dark-green [Pt(MCO)₂]_n and [Pt(PiPCO)₂]_n prompted us to investigate the photoluminescence of these compounds in the NIR range. To avoid the observed interconversion between the monomeric ↔ dimeric ↔ polymeric species in the solution (Scheme 3), we investigated the emission in the solid state. The solids were incorporated into the KBr matrix at 5% amounts to minimize the uncertainties associated with the powder density and particle size and enhance the reproducibility of the results. Such a technique is

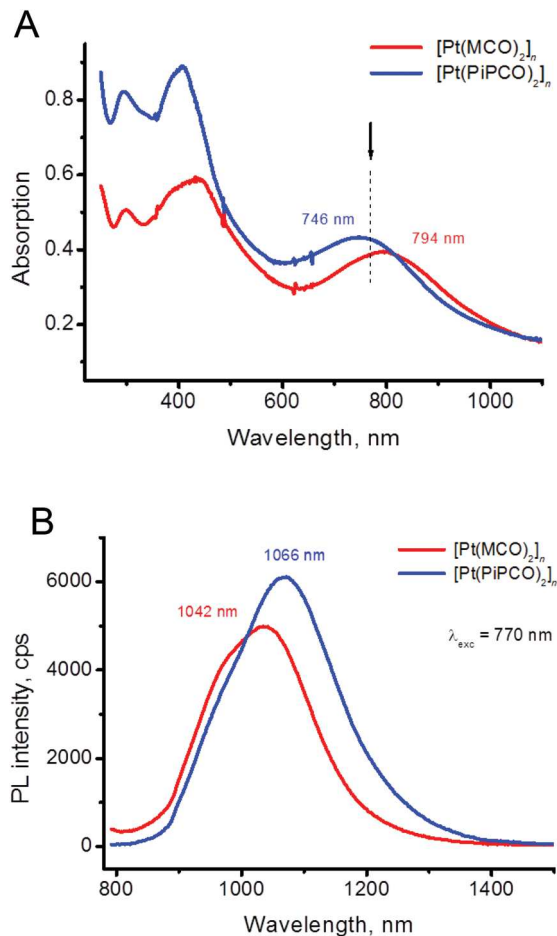


Fig. 5 A – Solid-state UV-visible spectra of dark-green 1D polymeric $[\text{Pt}(\text{PiPCO})_2]_n$ (blue) and $[\text{Pt}(\text{MCO})_2]_n$ (red) recorded as fine suspensions in silicone oil; the dotted line shows the excitation wavelength for recording emission spectra. B – Emission spectra of these compounds embedded in the KBr pellet at 5% by weight concentration.

commonly used in FTIR measurements,⁵⁷ but was originally also proposed for the absorption spectra in the past.⁴⁸ Also, we prepared KBr pellets with 1%, 0.5%, and 0.1% by weight of dark-green $[\text{Pt}(\text{MCO})_2]_n$ and $[\text{Pt}(\text{PiPCO})_2]_n$ complexes to investigate the effect of the concentration on the emission properties of polymers. Finally, we studied pure powdery samples of Pt-cyanoximate polymers to compare their emission with solid solutions in KBr pellets. Details of the pellet preparation as well as the used pure dark-green $[\text{Pt}(\text{MCO})_2]_n$ and $[\text{Pt}(\text{PiPCO})_2]_n$ compounds and experimental setup can be found in ESI 18 and 19.† The pellets had a long shelf-life stability (more than two years) if stored in a vacuum desiccator at room temperature. Crystalline IR-spectroscopy grade KBr was used to check any possible background emission stemming from the salt or the instrument (ESI 20–22†). We recently investigated the NIR emissive properties, or lack thereof, for control compounds, such as known model 1D Pt compounds with a known Pt...Pt distance – Magnus' Green Salt (MGS) and Krogman's Salt (partially oxidized tetracyano-platinate, POCP).⁴⁸

All pellets were excited at 770 nm with emission measured in the range of 800–1600 nm. The NIR photoluminescence spectra of $[\text{Pt}(\text{MCO})_2]_n$ and $[\text{Pt}(\text{PiPCO})_2]_n$ complexes (5% in KBr) are shown in Fig. 5B. The shape of the emission profile indicates a multicomponent emission for both complexes, and a satisfactory deconvolution of spectroscopic envelopes required only two Gaussian-type lines (ESI 71 and 72†). Two components, however, have significantly different parameters: line intensity, peak area and energy. This observation is somewhat similar to our recent finding for the NIR photoemission of another dark-green 1D polymer, $[\text{Pt}(\text{DECO})_2]_n$ (DECO[−] is the anion of 2-cyano-2-oximino-*N,N'*-dimethylacetamide), which has an almost symmetric emission profile at ~1060 nm,⁴⁸ but nevertheless fit for two Gaussian-type lines, but of a greatly different areas of 95 : 5. No vibronic progression is observable for the photoluminescence of $[\text{Pt}(\text{MCO})_2]_n$ and $[\text{Pt}(\text{PiPCO})_2]_n$ complexes. The emission–excitation scans for the KBr pellet with 5% content of both complexes are shown in Fig. 6 and

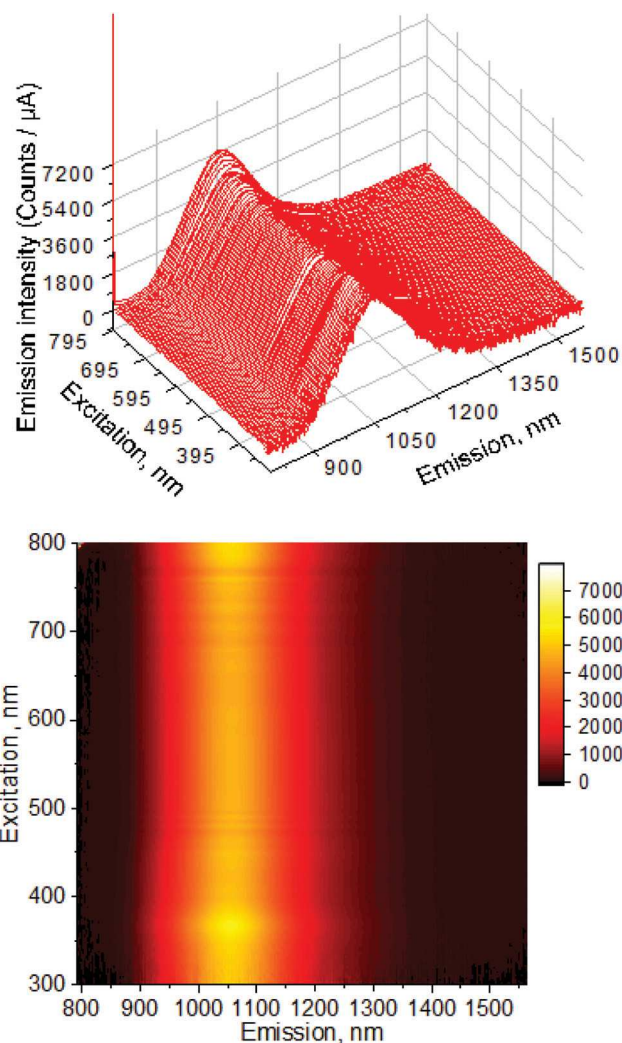


Fig. 6 The excitation spectra of dark-green 1D polymeric $[\text{Pt}(\text{MCO})_2]_n$ at 5% in the KBr pellet: top – 3D view; bottom – 2D map showing continuous emission at any excitation wavelength from 300 to 800 nm.

ESI 86† and evidenced that the position and intensity of the emission signal remain around ~ 1050 nm and is practically independent of the excitation wavelength. This is typical of systems with delocalized charge carriers such as mixed valence species, as well as quantum dots and quantum wells. In systems without charge delocalization excitation spectra have well-separated emission maximums, for example for the Nd-doped glass used for the instrument calibration (ESI 21†).

As expected, there is a pronounced concentration dependence of photoluminescence of $[\text{Pt}(\text{MCO})_2]_n$ and $[\text{Pt}(\text{PiPCO})_2]_n$ polymers in KBr pellets: (1) the intensity of the emission undergoes the bathochromic shift upon the increase of the complex's concentration (Fig. 7A), (2) the absolute quantum yield also increased significantly upon the complexes' dilution in the KBr matrix. The latter values are tabulated and plotted in ESI 77 and 78.† The data can be reasonably well fit using the mono-exponential decay function in ESI 79.† The plots of the intensities of the photoluminescence and values of quantum yield *versus* concentration are in line with the self-absorption of photons in more concentrated samples,^{67,68} while the red-shift of energy of the emission at higher concen-

trations is indicative of coupled oscillators where the total energy of the system decreases with the increase of their number.^{69,70} The PtL_2 ($L = \text{MCO}^-$, PiPCO^- anions) units connected *via* metal-lipophilic interactions are forming a long-range "metal wire" that provides such coupling. Moreover, the presence of mixed valency also contributed to the coupling since it provides more tight binding of PtL_2 subunits in a stack *via* an extended charge delocalization component shared between the electrons.

The life time measurements were carried out for 5% $[\text{PtL}_2]_n$ in KBr pellets and turned out to be in the nanoseconds range: $T_1 = 3.37 \times 10^{-9}$ and $T_2 = 1.26 \times 10^{-8}$ s (average time = 4.79×10^{-9} s) for $[\text{Pt}(\text{PiPCO})_2]_n$, and $T_1 = 2.73 \times 10^{-9}$ and $T_2 = 6.21 \times 10^{-9}$ s (average time = 3.45×10^{-9} s) for $[\text{Pt}(\text{MCO})_2]_n$ (ESI 83 and 84†). The values suggest the fluorescence nature of the observed photoemission for both polymers. We predict, however, that the life times would increase when such measurements will be carried out for the solutions of these complexes and aggregates in micelles, which we plan to conduct in the nearest future.

Control complexes such as well-known MGS and KCP, POCP embedded into salt pellets (5% in KBr) do not exhibit any NIR luminescence irrespective of the excitation wavelengths. Also, it should be noted that the yellow monomeric PtL_2 ($L = \text{MCO}$, PiPCO) complexes did not show any photoluminescence at all regardless of the wavelength of excitation. Therefore, the observed emission in the NIR region beyond 1000 nm is a collective property of self-assembled mixed valence 1D polymeric Pt-cyanoximates.

Variable temperature studies of photoemission were conducted for both the synthesized polymeric Pt-cyanoximate complexes and are shown in Fig. 8A and 9A. Deconvolution of the photoemission signals is shown in ESI 71 and 72,† while processed data of the line widths, intensities and areas at different temperatures are summarized in ESI 73–76.† There is a rather pronounced bathochromic shift in the energy of the photoemission for both components with the decrease of temperature. Thus, for the $[\text{Pt}(\text{MCO})_2]_n$ complex the energy that corresponds to the red-shift of 41 nm is 4.49 kJ mol^{-1} , or 46 meV (375 cm^{-1}) (Fig. 8A), while for the $[\text{Pt}(\text{PiPCO})_2]_n$ complex these values at the bathochromic shift of 48 nm are 3.97 kJ mol^{-1} , or 41 meV (332 cm^{-1}) (Fig. 9A). Both these values are typical of quantum dots and wells, which are semiconductors with free-moving charge carriers, and are also consistent with the delocalization of electrons along the 1D chain in compounds with metallophilic interactions.^{20,24,71}

The same trend was again observed for the peak intensity: the higher the temperature, the more intense the photoemission lines are (ESI 73-A and 75-A†). We reported similar behavior for the first representative of this new class of NIR emitters – another mixed valence dark-green 1D polymer, $[\text{Pt}(\text{DECO})_2]_n$ ($\text{DECO} = 2\text{-cyano-2-oximino-}N,N'\text{-dimethylacetamide}$).⁴⁸ We explain the simultaneous increase in the emission intensity with temperature by analogy with the documented behavior of quantum wells (single quantum wells GaAsSb/AlGaAs) and quantum dots (multi-core and multi-shell CdSe/CdS/ZnS/ZnSe) with delocalized carriers typical of semi-

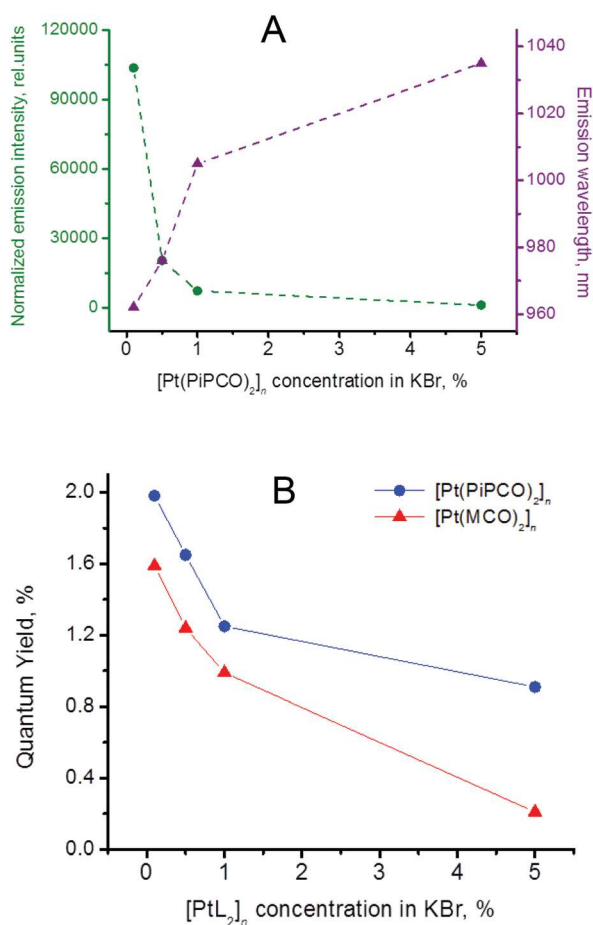


Fig. 7 The concentration effect of the emission intensity vs. its wavelength in KBr pellets with embedded $[\text{Pt}(\text{PiPCO})_2]_n$ (A), and the absolute quantum yield of both studied 1D polymeric Pt-cyanoximates vs. complex concentration in pellets (B).

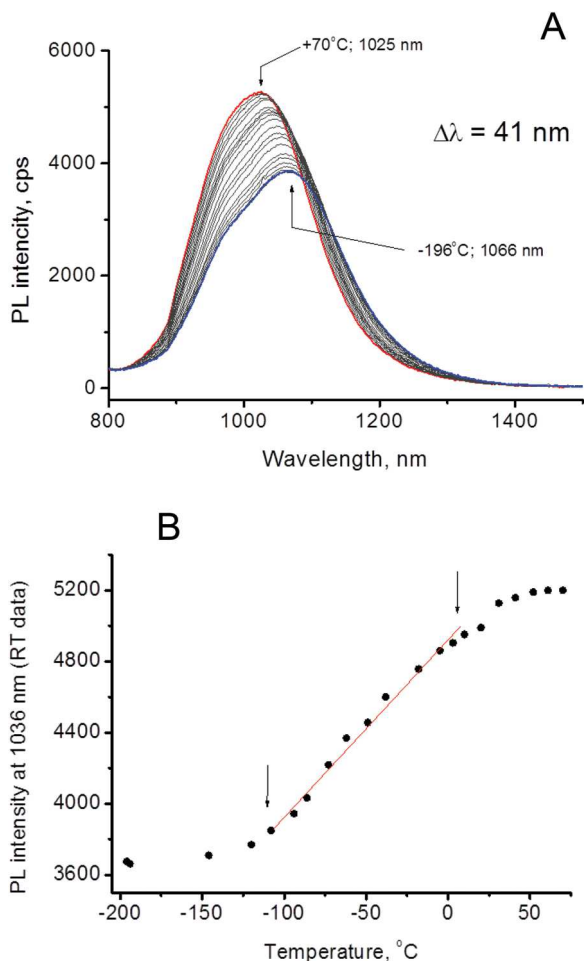


Fig. 8 Variable temperature photoluminescence of 1D dark-green polymeric $[\text{Pt}(\text{MCO})_2]_n$ embedded into the KBr matrix at 5% concentration (A), and s-shaped response of emission intensity to the temperature change (B). A "linear part" can be approximated as indicated by arrows.

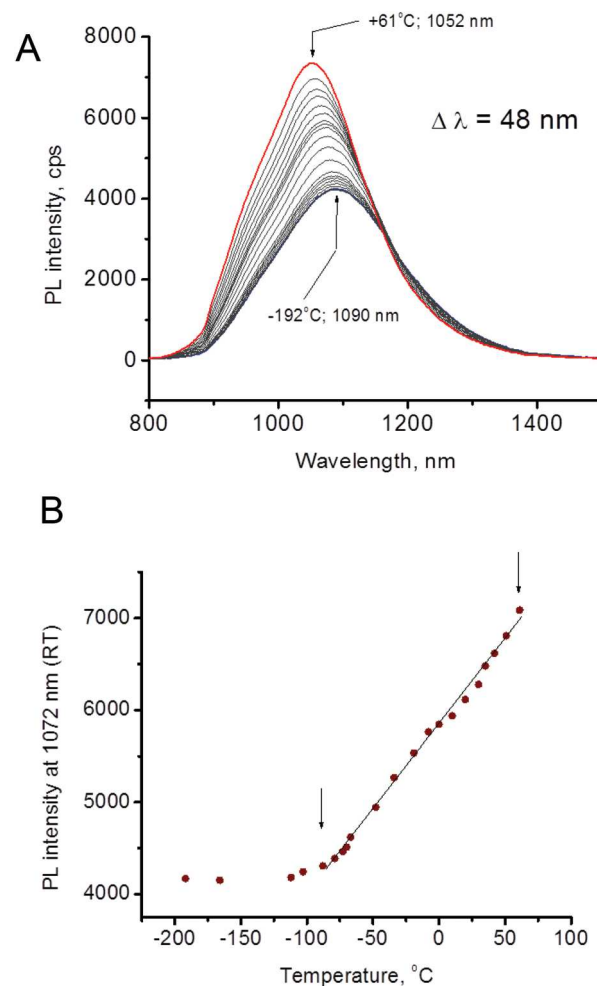


Fig. 9 Variable temperature photoluminescence of 1D dark-green polymeric $[\text{Pt}(\text{PiPCO})_2]_n$ embedded into the KBr matrix at 5% concentration (A), and a large range of linear responses (indicated by arrows) of emission intensity to the temperature change (B).

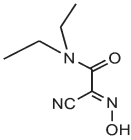
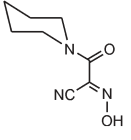
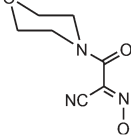
conductors. Both demonstrate similar temperature-induced changes in the emission energies and intensity profiles. Subsequently, excitons with a temperature increase gain sufficient thermal energy to overcome small potential barriers in the local potential minimum, become mobile, and transferred to higher energy states of the band until reaching the edge of the conduction band.^{72,73} Therefore, the emission energy undergoes a blue shift with the increase of temperature. We propose that at the low temperatures reached in our experiments, excitons mostly localize in a mixed valence aggregate which is small in size, or perhaps even in the mixed valence dimer. Also, the thermal lattice contraction caused by cooling results in shorter Pt...Pt distance in stacks, which leads to the red shift.⁷⁴ The increase of the temperature creates delocalized excitons that can now reach higher energy states and, due to electron hopping, spread over a larger distance, increasing the probability of emission from a larger number of mixed valence centers along the Pt...Pt wire.

The metal-metal distance is increased with temperature as well. In general, the increasing with temperature hopping of pairs of electrons between sites leads to a greater degree of delocalization in both ground and excited states.⁷⁵ Lastly, these results can also be explained in terms of the increase of the distance traveled by electrons along the 1D Pt...Pt chain (e-delocalization) with the rising temperature, which requires higher energy. Lower temperatures tend to localize such motion to a smaller distance. Similar blue-shift behavior was reported for a series of In-As quantum dots⁷⁶ and wells⁷² and Cd-chalcogenide^{77,78} where even values of the PL temperature shifts were reported to be in the same range of 30–60 meV.

It is interesting to note in the context of our observation of emission beyond 900 nm in $[\text{PtL}_2]_n$ that the oxidation of Pt(II) to Pt(III) in several As-Pt and phosphite-Pt dimers also leads to a significant red shift in the emission.⁹¹

The plots of the emission intensity of the signal from the temperature showed considerable linear parts for both the studied 1D polymeric Pt-cyanoximates (Fig. 8B, 9B; Table 5).

Table 5 Comparison of the photophysical properties of the studied dark-green 1D polymeric Pt-cyanoximates embedded into a KBr matrix at 5 wt% concentration. All data were collected at 770 nm excitation wavelength

Complex	Cyanoxime	Variable temperature measurements					
		λ_{max} emissions	$\Delta\lambda$, nm/ cm ⁻¹ /meV	Effect of VT on signals	Linear <i>T</i> range, °	QY, %	Ref.
[Pt(DECO) ₂] _n		One band; 1043 nm (+67 °C) 1097 nm (-175 °C)	54/472/58	hypsochromic shift with temperature increase; intensity decrease with temperature decrease	~115	0.51	48
[Pt(PiPCO) ₂] _n		Two overlapping bands ^a Centered at 1052 nm (at +61 °C) Centered at 1090 nm (at -192 °C)	48/332/41	The same as above	~140	0.91	This work
[Pt(MCO) ₂] _n		Two overlapping bands ^b Centered at 1025 nm (at +70 °C) Centered at 1066 nm (at -196 °C)	41/375/47	The same as above	~98	0.21	This work

^a Details can be seen in ESI 83. ^b And in ESI 82.

These are ~98° in length for [Pt(MCO)₂]_n (between -108° and +10 °C), and ~140° in length for [Pt(PiPCO)₂]_n (between -80 and +60 °C) (ESI 69 and 70†). The slope for the [Pt(PiPCO)₂]_n is about twice as steep as that for the linear part of [Pt(MCO)₂]_n, but both are significantly smaller than the linear part of the recently published [Pt(DECO)₂]_n.⁴⁸ Such long linear parts of the PL intensity of this new class of 1D polymeric Pt-cyanoximates can be used for non-electrical, optical thermometers working in the NIR region.

Micelles of both polymeric [Pt(MCO)₂]_n and [Pt(PiPCO)₂]_n complexes display photoluminescence at almost the same wavelength beyond 1000 nm as solid samples. These complexes have shown pronounced cytotoxicity,³⁶⁻³⁸ which makes them interesting for application as theranostic agents. Thus, recently we found that the [Pt(MCO)₂]_n complex being mixed with the anticancer drug Ganetespib and formulated in micelles with the Fe(III)-containing polymer of nanoparticle size significantly enhances the cytotoxicity of the drug.⁷⁹

Practicality of mixed valence "Pt-wires"

Micelle formation

Also, we performed solubilization of solid polymeric [Pt(MCO)₂]_n and [Pt(PiPCO)₂]_n complexes into aqueous solutions with the help of ultrasound and detergents such as sodium decanoate and sodium dodecylsulfate. Both complexes form dark-green micelle solutions (ESI 53 and 54†), which after filtration were examined by the DLS method. It was a surprise to see that [Pt(MCO)₂]_n and [Pt(PiPCO)₂]_n form homogeneous, single particle size colloidal solutions, which turned out to be stable within a month. Thus, the first complex forms micelles with an average size of 322.5 nm and, using the Pt...Pt bond = 3.15 Å in the polymer (determined by the EXAFS method), there are ~920 units in the stack. A similar evaluation for average single-size particles of 214.1 nm for [Pt(PiPCO)₂]_n micelles resulted in ~680 units in the stack. Data of elevated total Pt content determination in micelles of both complexes evidenced that the latter contain clearly more than one stack.

NIR imaging

With the use of a special Ninnox camera sensitive in the NIR region, we were able to record actual images of both pure powders of polymeric [Pt(MCO)₂]_n and [Pt(PiPCO)₂]_n complexes as well as their 5% by weight solid solutions in KBr (Fig. 10). The KBr pellet with 5% of Krogman's salt (partially oxidized KCP) was used as a non-luminescent control (Fig. 10C and D). Both type of samples – powders and pellets – were photographed under ambient conditions using white light (Fig. 10A and C). Images in the NIR region were recorded using 735 nm excitation with a bright LED source with 0.5 s exposure time and a long-path 800 nm filter that blocks all light with wavelength less than 800 nm. Good quality images of the studied samples emitting in the NIR region beyond 1000 nm (shown in Fig. 10B and D) were recorded for the coordination polymers for the first time ever. Photographs of four un-illuminated KBr pellets under excitation with 735 nm LED light, with different concentrations (0.1%, 0.5%, 1% and 5%) of [Pt(MCO)₂]_n, are shown in ESI 85.† Then the image of the same pellets illuminated at the above wavelength shows them to be clearly visible and brightly colored. In addition, the Petri dish

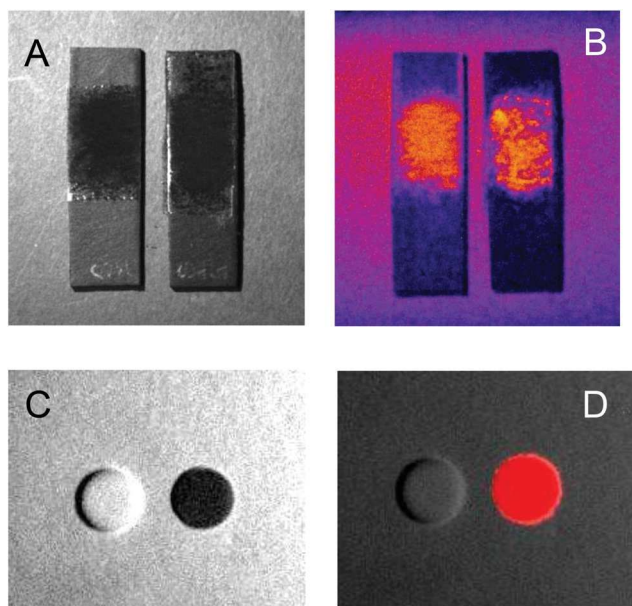


Fig. 10 Images of pure powders of dark-green 1D-polymeric Pt-cyanoximates (on double-sided transparent adhesive tape attached to a black cardboard) recorded with the help of a Ninnox image camera. The left panel corresponds to $[\text{Pt}(\text{MCO})_2]_n$, and the right one to $[\text{Pt}(\text{PiPCO})_2]_n$. A – “as is” images recorded under ambient conditions; B – the same panels recorded using 735 nm excitation with a LED source; C – KBr pellets with 5% embedded compounds; left – partially oxidized KCP (Krogman’s salt) and right – $[\text{Pt}(\text{PiPCO})_2]_n$; D – the same pellets photographed using 735 nm excitation with a LED source with 0.5 s exposure time and a long-path 800 nm filter.

with water was placed over two pellets to show that the NIR emission from the complex is not obstructed by water. This is important for future experiments with cell cultures and biological tissue aimed at the theranostic application of these NIR emitters.

Conclusions

- The reaction of the K^+ salts of the two *N*-substituted-acetamide cyanoxime anions PiPCO^- and MCO^- with K_2PtCl_4 led to the formation of complexes of PtL_2 composition which exist as at least two polymorphs: monomeric yellow complexes and dark-green $[\text{PtL}_2]_n$ 1D polymers in which individual PtL_2 units are held together *via* $\text{Pt}\cdots\text{Pt}$ metallophilic interactions.

- The cyanoxime ligands used in these preparations are inexpensive compounds that are easily produced in one step from commercially available precursors that form Pt-complexes in a good yield. This is contrary to the much more difficult to obtain and purify other known heterocyclic ligands and organometallic Pt-complexes that are typically used in these studies. Yet, the polymeric $[\text{Pt}(\text{MCO})_2]_n$ and $[\text{Pt}(\text{PiPCO})_2]_n$ compounds presented in this work outperform in the NIR emission wavelengths all previously reported “Pt-wires”.

- Current work opens a new page in studies of mixed donor 1D solids with $[\text{PtN}_2\text{O}_2]$ inner coordination spheres with by far

more interesting chemical and physical properties such as better solubility in common solvents, photoluminescence and solid state semiconductivity.

- The obtained solid $[\text{Pt}(\text{MCO})_2]_n$ and $[\text{Pt}(\text{PiPCO})_2]_n$ 1D polymers represent “metal wires” since they demonstrate a relatively high electrical conductivity ($20\text{--}30\text{ S cm}^{-1}$ = semiconductors) which is typical of a mixed valence species. There is a small amount of Pt(IV) species in these complexes, sufficient for the facilitation of electron hopping between Pt(II) and Pt(IV) centers. Tetravalent platinum could be partially generated either aerobically by oxygen from the air or *via* oxidation of the metal with the cyanoxime or *via* disproportionation of the initial Pt(II) species to Pt(0) and Pt(IV) complexes or due to catalytically generated products of further chemical modifications of cyanoximes that lead to partial generation of Pt(IV) species.

- Being dissolved in solvents that do not disrupt the metallophilic interactions in stacks these complexes spontaneously aggregate to form opaque colloidal systems with single-size particles that contain ~ 920 (for $[\text{Pt}(\text{MCO})_2]_n$) and ~ 680 (for $[\text{Pt}(\text{PiPCO})_2]_n$) units per stack.

- The same 1D polymeric complexes also show a rather intense NIR fluorescence beyond 1000 nm. At the same time, yellow monomeric PtL_2 are not emissive, which evidences the importance of the aggregation and the metallophilic interaction for the fluorescence.

- The chemical oxidation of $[\text{Pt}(\text{MCO})_2]_n$ and $[\text{Pt}(\text{PiPCO})_2]_n$ in solutions and in the solid state increases the intensity of the MMLCT band in the visible region of the spectrum and increases the NIR emission intensity.

- The photoluminescence of both 1D polymeric Pt-cyanoximates in an ionic salt matrix (KBr) increases with the concentration of the complex decrease, with quantum yields being in the range between 0.2 and 2%.

- The photoluminescence of 1D polymers at 5% concentration in KBr at variable temperatures showed a very pronounced bathochromic shift of the emission λ_{max} and an intensity decrease with lowering temperature, similarly to some semiconductor-based confined quantum dots and wells. Our work with polymeric dark-green Pt-cyanoximates at variable temperatures represents the first observation of this kind of emission behavior in these mixed valence “metal wires”.

- Images of pure solid powders of $[\text{Pt}(\text{MCO})_2]_n$ and $[\text{Pt}(\text{PiPCO})_2]_n$ samples as well as in dilute KBr matrices emitting in the NIR region beyond 1000 nm were recorded for the first time.

- The demonstrated photoluminescence of the studied 1D complexes combined with the established compounds’ cytotoxicity makes them interesting candidates for theranostic applications.

Conflicts of interest

There are no conflicts to declare. Reported in this paper two Pt-cyanoximates and their polymorphs are a subject of the U.S. Patent Application “Near Infrared Emitters” under US Patent Application No. 15/001,023 filed on January 19, 2016. Status: pending.

Acknowledgements

NG is very grateful to the following individuals for their help during work on this project: Dr Dan Zhou from the University of Missouri – St Louis for the recording of SEM images; Prof. Dennis Tallman from North Dakota State University for his help with the electrical conductivity measurements of powdery Pt-cyanoximate samples using the AFM method; Dr Allen Oliver (Notre Dame University) and Dr Jeannette Krause (University of Cincinnati) for data collection on the synchrotron source at UC-Berkeley, whereas the Advanced Light Source is supported by the U.S. Department of Energy, Office of Basic Energy Sciences, Materials Sciences Division, under contract DE-AC02-05CH11231. Ng is also grateful to Prof. Vlad Kolesnichenko from Xavier University of Louisiana for his initial help with the assessment of particle size in Pt-cyanoximates systems; Prof. Vivian Yam from Hong-Kong University for her help with the initial measurements of photoemission of two Pt-cyanoximates in solutions; Dr Jim Matheis from Horiba for the determination of the NIR emission lifetimes for both Pt-cyanoximates in the solid state; Ms Hanna Roda for her kind help with the electrochemical measurements of the solutions; and Ms Alexandra Corbett for invaluable technical assistance during the manuscript preparation. We also acknowledge MSU Graduate College for partial financial support of this work throughout several years, and the financial support from the NCI/NIH (R21CA149814) and NSF (1355466). We also thank the Washington University Optical Spectroscopy Core Facility (NIH 1S10RR031621-01) for spectroscopy measurements. We are grateful to Dr Justin Douglas from the University of Kansas for recording the EPR spectra of solid samples (support for the EPR instrumentation was provided by NSF Chemical Instrumentation Grant No. 0946883). VNN is grateful for the NSF support with the MRI-1420373 award for acquisition of the mass spectrometer.

References

- L. H. Doerr, *Comments Inorg. Chem.*, 2008, **29**, 93.
- J. Berry, *Extended metal atoms chains*, Springer Science and Business Media, Inc., 3rd edn, 2005.
- P. Day, N. S. Hush and R. J. H. Clark, *Philos. Trans. R. Soc., A*, 2008, **366**, 5.
- M. B. Robin and P. Day, *Adv. Inorg. Chem. Radiochem.*, 1967, **10**, 247.
- P. Day, *Mixed-valence Compounds*, Reidel, Dordrecht, 1980, vol. 58, p. 3.
- G. C. Allen and N. S. Hush, *Intervallence-transfer absorption. I. Qualitative evidence for intervalence-transfer absorption in inorganic systems in solution and in the solid state*, 1967, vol. 8.
- N. S. Hush, *Intervallence-transfer absorption. Part 2. Theoretical considerations and spectroscopic data*, 1967, vol. 8.
- J. P. Fackler, *Mixed Valence Compounds*, John Wiley & Sons, England, 2006.
- R. H. Terril and R. W. Murray, *Electron hopping transport in electrochemically active, molecular mixed valent materials*, Blackwell Science, Hoboken, NJ, USA, 1997.
- K. Krogmann, *Angew. Chem., Int. Ed. Engl.*, 1969, **8**, 35.
- N. Kojima, F. Fukuhara, H. Kitagawa, H. Takahashi and N. Mōri, *Synth. Met.*, 1997, **86**, 2175.
- J.-M. Bret, P. Castan and J.-P. Laurent, *Inorg. Chim. Acta*, 1981, **51**, 103.
- J. S. Miller and A. J. Epstein, *Prog. Inorg. Chem.*, 1976, **20**, 1.
- N. Tancret, S. Obbade, N. Bettahar and F. Abraham, *J. Solid State Chem.*, 1996, **124**, 309.
- N. Kimura, S. I. Ishimaru, R. Ikeda and M. Yamashita, *J. Chem. Soc., Faraday Trans.*, 1998, **94**, 3659.
- C. M. De Sadeleer, V. P. Hanot and T. D. Robert, *Transition Met. Chem.*, 1994, **19**, 585.
- H. J. Keller, in *Extended Linear Chain Compounds*, ed. J. S. Miller, Plenum Press, New York, 1983, vol. 1, p. 357.
- B. Scott, B. L. Bracewell, S. R. Johnson, B. I. Swanson, J. F. Bardeau, A. Bulou and B. Hennion, *Chem. Mater.*, 1996, **8**, 321.
- J. A. Brozik, B. L. Scott and B. I. Swanson, *J. Phys. Chem. B*, 1999, **103**, 10566.
- G. C. Stevens, *Platinum Met. Rev.*, 1979, **23**, 23.
- J. M. Williams, A. J. Schultz, A. E. Underhill and K. Carneiro, The Synthesis, Structure, Electrical Conduction Properties, and Theory of Divalent, Tetravalent, and One-Dimensional Partially Oxidized Tetracyanoplatinate Complexes, in *Extended Linear Chain Compounds*, ed. J. S. Miller, Springer US, Plenum Press NY, 1982, pp. 73–118.
- A. E. Underhill, D. M. Watkins, J. M. Williams and K. Carneiro, Linear Chain Bis(oxalato)platinate Salts, in *Extended Linear Chain Compounds*, ed. J. Miller, Springer US, Plenum Press, NY, 1982, pp. 119–156.
- A. E. Underhill, D. M. Watkins and C. S. Jacobsen, *Solid State Commun.*, 1980, **36**, 477.
- M. Mégnamisi-Béloméé, *J. Solid State Chem.*, 1979, **27**, 389.
- J. W. Brill, M. Mégnamisi-Béloméé and M. Novotny, *J. Chem. Phys.*, 1978, **68**, 585.
- T. Yamaguchi, N. Nishimura, K.-I. Shirakura and T. Ito, *Bull. Chem. Soc. Jpn.*, 2000, **73**, 775.
- M. Kanakubo, K. Yamamoto, K. Honda, H. Ushijima, T. Kamata, F. Mizukami and T. Ohta, *Anal. Sci.*, 1999, **15**, 107.
- H. Endres, H. J. Keller, H. van de Sand and V. Dong, *Z. Naturforsch.*, 1978, **33b**, 843.
- G. Ferraris and D. Viterbo, *Acta Crystallogr., Sect. B: Struct. Crystallogr. Cryst. Chem.*, 1969, **25**, 2066.
- J. L. Brianoso and M. de Matheus, *Afinidad*, 1982, **39**, 271.
- K. Matsumoto and K. Sakai, *Adv. Inorg. Chem.*, 1999, **49**, 375.
- T. Abe, H. Moriyama and K. Matsumoto, *Inorg. Chem.*, 1991, **30**, 4198.
- K. Sakai and K. Matsumoto, *J. Am. Chem. Soc.*, 1989, **111**, 3074.
- T. V. O'Halloran, P. K. Mascharak, I. D. Williams, M. M. Roberts and S. J. Lippard, *Inorg. Chem.*, 1987, **26**, 1261.
- B. Lippert, H. Schoellhorn and U. Thewalt, *Inorg. Chem.*, 1987, **26**, 1736.

- 36 D. Eddings, C. Barnes, N. Gerasimchuk, P. Durham and K. Domasevich, *Inorg. Chem.*, 2004, **43**, 3894.
- 37 N. Gerasimchuk, L. Goeden, P. Durham, C. Barnes, J. F. Cannon, S. Silchenko and I. Hidalgo, *Inorg. Chim. Acta*, 2008, **361**, 1983.
- 38 J. Ratcliff, P. Durham, M. Keck, A. Mokhir and N. Gerasimchuk, *Inorg. Chim. Acta*, 2012, **385**, 11.
- 39 Y. Liu, A. Q. Bauer, W. J. Akers, G. Sudlow, K. Liang, D. Shen, M. Y. Berezin, J. P. Culver and S. Achilefu, *Surgery*, 2011, **149**, 689.
- 40 S. L. Troyan, V. Kianzad, S. L. Gibbs-Strauss, S. Gioux, A. Matsui, R. Oketokoun, L. Ngo, A. Khamene, F. Azar and J. V. Frangioni, *Ann. Surg. Oncol.*, 2009, **16**, 2943.
- 41 N. G. Zhegalova, G. Gonzales and M. Y. Berezin, *Org. Biomol. Chem.*, 2013, **11**, 8228.
- 42 D. Salo, H. Zhang, D. M. Kim and M. Y. Berezin, *J. Biomed. Opt.*, 2014, **19**, 086008.
- 43 B. E. Schaafsma, J. S. Mieog, M. Hutteman, J. R. van der Vorst, P. J. Kuppen, C. W. Lowik, J. V. Frangioni, C. J. van de Velde and A. L. Vahrmeijer, *J. Surg. Oncol.*, 2011, **104**, 323.
- 44 P. W. Barone, S. Baik, D. A. Heller and M. S. Strano, *Nat. Mater.*, 2005, **4**, 86.
- 45 M. W. Knight, H. Sobhani, P. Nordlander and N. J. Halas, *Science*, 2011, **332**, 702.
- 46 G. Qian, Z. Zhong, M. Luo, D. Yu, Z. Zhang, Z. Y. Wang and D. Ma, *Adv. Mater.*, 2009, **21**, 111.
- 47 N. Gerasimchuk, M. Berezin and D. R. Klaus, in 1D coordination polymers based on Pt(II) cyanoximates as new class of NIR emitters beyond 900 nm, 49th Midwest Regional Meeting of the American Chemical Society, Columbia, MO, USA, November 15–16, 2014, 2014, Columbia, MO, USA, 2014, pp Oral presentation, #308.
- 48 D. R. Klaus, M. Keene, S. Silchenko, M. Berezin and N. Gerasimchuk, *Inorg. Chem.*, 2015, **54**, 1890.
- 49 J. Ratcliff, J. Kuduk-Jaworska, H. Chojnacki, V. Nemykin and N. Gerasimchuk, *Inorg. Chim. Acta*, 2012, **385**, 1.
- 50 A. Mann, N. Gerasimchuk and S. Silchenko, *Inorg. Chim. Acta*, 2016, **440**, 118.
- 51 W. Ostwald, *Z. Phys. Chem.*, 1897, **22**, 289.
- 52 H. Matschiner, H. Kohler and R. Matuschke, *Z. Anorg. Allg. Chem.*, 1971, **380**, 267.
- 53 A. A. Mokhir, K. V. Domasevich, N. Kent Dalley, X. Kou, N. N. Gerasimchuk and O. A. Gerasimchuk, *Inorg. Chim. Acta*, 1999, **284**, 85.
- 54 D. Marcano, N. Gerasimchuk, V. Nemykin and S. Silchenko, *Cryst. Growth Des.*, 2012, **12**, 2877.
- 55 N. Gerasimchuk, A. N. Esaulenko, K. N. Dalley and C. Moore, *Dalton Trans.*, 2010, **39**, 749.
- 56 H. Köhler and G. Lux, *Inorg. Nucl. Chem. Lett.*, 1968, **4**, 133.
- 57 A. Gordon and R. Ford, *The Chemist's Companion: A Handbook of Practical Data, Techniques, and References*, John Wiley & Sons, New York, London, Sydney, Toronto, 1972.
- 58 J. A. Dean, *Lange's Handbook of Chemistry*, Mc Graw-Hill, 1999.
- 59 *CRC Handbook of Chemistry and Physics*, Taylor & Francis Ltd, 96th edn, 2015, p. 2677.
- 60 B. G. Anex, *J. Chem. Phys.*, 1967, **46**, 1090.
- 61 J. R. Miller, *J. Chem. Soc.*, 1965, **44**, 713.
- 62 B. Morosin, P. Fallon and J. S. Valentine, *Acta Crystallogr., Sect. B: Struct. Crystallogr. Cryst. Chem.*, 1975, **31**, 2220.
- 63 C. N. Riddles, M. Whited, S. R. Lotlikar, K. Still, M. Patrauchan, S. Silchenko and N. Gerasimchuk, *Inorg. Chim. Acta*, 2014, **412**, 94.
- 64 A. A. Mokhir, K. V. Domasevich, N. Kent Dalley, X. Kou, N. N. Gerasimchuk and O. A. Gerasimchuk, *Inorg. Chim. Acta*, 1999, **284**, 85.
- 65 N. Gerasimchuk and N. K. Dalley, *J. Coord. Chem.*, 2004, **57**, 1431.
- 66 H. Endres, H. J. Keller, H. van de Sand and Vu Dong, *Z. Naturforsch.*, 1978, **33b**, 843.
- 67 X.-F. Zhang, Q. Xi and J. Zhao, *J. Mater. Chem.*, 2010, **20**, 6726.
- 68 N. N. Gerasimchuk, A. A. Mokhir and K. R. Rodgers, *Inorg. Chem.*, 1998, **37**, 5641.
- 69 L. Zhou, n-coupled oscillator, in *Mathematics course FICI 1039*, University de Los Andes, 2012, p. 1.
- 70 R. B. Martin, *Chem. Rev.*, 1996, **96**, 3043.
- 71 T. W. Thomas and A. E. Underhill, *Chem. Soc. Rev.*, 1972, **1**, 99.
- 72 S. A. Lourenco, I. F. L. Dias, J. L. Duarte, E. Laureto, V. M. Aquino and J. C. Harmand, *Braz. J. Phys.*, 2007, **37**, 1212.
- 73 P. Jing, J. Zheng, M. Ikezawa, X. Liu, S. Lv, X. Kong, J. Zhao and Y. Masumoto, *J. Phys. Chem. C*, 2009, **113**, 13545.
- 74 D. E. Janzen, M. Pomije, C. A. Daws, C. L. Exstrom and K. R. Mann, Vaporochromic platinum complexes and salts, *US patent 5766952*, 1998.
- 75 W. E. Buschmann, S. D. McGrane and A. P. Shreve, *J. Phys. Chem. A*, 2003, **107**, 8198.
- 76 H. J. Park, J. H. Kim, H. H. Ryu, M. Jeon, J. Y. Leem, J. S. Kim, J. S. Kim, J. S. Son and D. Y. Lee, *J. Korean Phys. Soc.*, 2007, **51**, 1383.
- 77 T. T. K. Chi, N. Q. Liem, M. H. Nam and D. X. Thanh, *J. Korean Phys. Soc.*, 2008, **52**, 1510.
- 78 N. Bel Haj Mohamed, M. Haouari, Z. Zaaboub, M. Nafoutti, F. Hassen, H. Maaref and H. Ben Ouada, *J. Nanopart. Res.*, 2014, **16**, 2242.
- 79 J. Kallu, T. Banerjee, S. Sulthana, B. Heckert, N. Gerasimchuk and S. Santra, Oral presentation, 183 In Hsp90 inhibitor carrying magnetic nanotheranostics for the treatment of non-small-cell lung cancer., 50th Midwest Regional ACS meeting, St. Joseph, Missouri, USA, October 21–24, 2015, St. Joseph, Missouri, USA, 2015, pp 183, oral presentation.
- 80 M. Sakhawat Hussain, B. E. V. Salinas and E. O. Schlemper, *Acta Crystallogr., Sect. B: Struct. Sci.*, 1979, **35**, 628.
- 81 J. R. Stork, M. M. Olmstead, J. C. Fettinger and A. L. Balch, *Inorg. Chem.*, 2006, **45**, 849.
- 82 G. Aullón and S. Alvarez, *Eur. J. Chem.*, 1997, **3**, 655.
- 83 T. Yamaguchi, N. Nishimura and T. Ito, *J. Am. Chem. Soc.*, 1993, **115**, 1612.
- 84 L. A. M. Baxter, G. A. Heath, R. G. Raptis and A. C. Willis, *J. Am. Chem. Soc.*, 1992, **114**, 6944.

- 85 H. Endres, *Acta Crystallogr., Sect. C: Cryst. Struct. Commun.*, 1985, **41**, 1047.
- 86 H. Endres and L.-B. Gelb, *Z. Naturforsch.*, 1986, **41b**, 137.
- 87 V. M. Miskowski and V. H. Houlding, *Inorg. Chem.*, 1989, **28**, 1529.
- 88 J. K. Seong and G. Ehrlich, *Phys. Rev. B: Condens. Matter*, 2000, **62**, R10645(R).
- 89 V. M. Miskowski and V. H. Houlding, *Inorg. Chem.*, 1991, **30**, 4446.
- 90 K. Li, G. So Mi Tong, Q. Wan, G. Cheng, W.-Y. Tong, W.-H. Ang, W.-L. Kwong and C.-M. Che, *Chem. Sci.*, 2016, **7**, 1653.
- 91 M. A. Bennett, S. K. Bhargava, C.-C. E. Cheng, W. H. Lam, T. K.-M. Lee, S. H. Priver, J. Wagler, A. C. Willis and V. W.-W. Yam, *J. Am. Chem. Soc.*, 2010, **132**(20), 7094.
- 92 K. T. Ly, R.-W. Chen-Cheng, H.-W. Lin, Y.-J. Shiau, S.-H. Liu, P.-T. Chou, C.-S. Tsao, Y.-C. Huang and Y. Chi, *Nat. Photonics*, 2017, **11**, 63.
- 93 N. Gerasimchuk and M. Berezin, A new strategy for the NIR emitters beyond 900 nm: preparation of self-assembled luminescent 1D Pt-cyanoximates, Abstract of Papers, 250th ACS National Meeting, Boston, MA, August 16–20, 2015, INOR-595; oral presentation.
- 94 (a) V. Y. Kukushkin, V. K. Belsky and D. Tudela, *Inorg. Chem.*, 1996, **35**(2), 510; (b) D. Bolotin, M. Y. Demakova, A. S. Novikov, M. S. Avdontceva, M. L. Kuznetsov, N. A. Bokach and V. Y. Kukushkin, *Inorg. Chem.*, 2015, **54**(8), 4039; (c) A. I. Mikhaleva, A. B. Zaitsev and B. A. Trofimov, *Russ. Chem. Rev.*, 2006, **75**(9), 797.
- 95 (a) M. L. Kuznetsov, N. A. Bokach, V.Y. Kukushkin, T. Pakkanen, G. Wagner and A. J. L. Pombeiro, *J. Chem. Soc., Dalton Trans.*, 2000, **24**, 4683–4693; (b) V. Y. Kukushkin, D. Tudela and A. K. L. Pombeiro, *Coord. Chem. Rev.*, 1996, **156**, 333.